JACS JOURNAL OF THE AMERICAN CHEMICAL SOCIETY

pubs.acs.org/JACS Article

From Carbodiimides to Carbon Dioxide: Quantification of the Electrophilic Reactivities of Heteroallenes

Zhen Li, Robert J. Mayer, Armin R. Ofial,* and Herbert Mayr*

Cite This: https://dx.doi.org/10.1021/jacs.0c01960 Read Online

ACCESS | Metrics & More | Article Recommendations | Supporting Information

ABSTRACT: Kinetics of the reactions of isocyanates, isothiocyanates, carbodiimides, carbon disulfide, and carbon dioxide with carbanions or enamines (reference nucleophiles) have been measured photometrically in acetonitrile or DMSO solution at 20 °C. The resulting second-order rate constants and the previously published reactivity parameters N and s_N of the reference nucleophiles were substituted into the correlation $\log k_2(20\ °C) = s_N(N + E)$ to determine the electrophilicity parameters of the heteroallenes: TsNCO ($E = -7.69$) ≫ PhNCO ($E = -15.38$) > CS_2 ($E = -17.70$) ≈ PhNCS ($E = -18.15$) > PhNCNPh ($E = -20.14$) ≫ CyNCNCy ($E \approx -30$). An approximate value could be derived for CO_2 ($-16 < E < -11$). Quantum chemical calculations were performed at the IEFPCM(DMSO)/B3LYP-D3/6-311+G(d,p) level of theory and compared with experimental Gibbs activation energies. The distortion−interaction model was used to rationalize the different reactivities of O- and S-substituted heteroallenes. Eventually it is demonstrated that the electrophilicity parameters determined in this work can be used as ordering principle for literature-known reactions of heteroallenes.

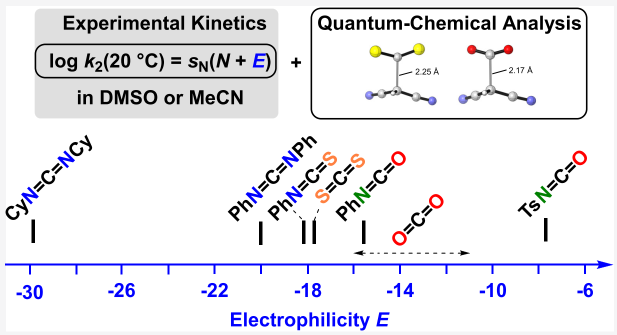

INTRODUCTION

Heteroallenes[1] are important reagents in organic synthesis; they include isocyanates,[2] isothiocyanates,[2d,3] carbodiimides,[4] carbon disulfide,[5] carbon dioxide,[6] etc. Whereas isocyanates, in particular those with electron-withdrawing substituents, are known to be highly reactive electrophiles,[2c,g,h] carbon dioxide is a rather inert molecule, and many attempts to use it as a feedstock for organic compounds are presently investigated.[7] It was the goal of this work to elucidate relationships between structure and reactivities of heteroallenes (Chart 1) in order to include these compounds in our comprehensive electrophilicity scales and in this way describe their applicability in organic synthesis.

In previous work, we had developed scales of nucleophilicity and electrophilicity on the basis of eq 1, which can be used to predict scope and selectivities of reactions of a large variety of electrophiles with π-, σ-, and n-nucleophiles. The linear free-energy relationship (1) characterizes electrophiles by one parameter (electrophilicity E) and nucleophiles by two solvent-dependent parameters (nucleophilicity N and susceptibility s_N).[8]

$$\log k_2(20\ °C) = s_N(N + E) \quad (1)$$

We now report on the kinetics of the reactions of the heteroallenes **1a−1h** with the carbanions **2** and enamines **3** (Table 1)[9] and use the resulting rate constants for determining the electrophilicity parameters E of **1a−1h**.

Chart 1. Heteroallenes 1a−1h Studied in This Work (Cy = Cyclohexyl)

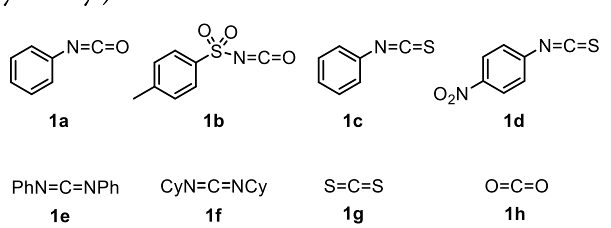

RESULTS AND DISCUSSION

Product Studies. The reactions of the heteroallenes **1** with the reference nucleophiles **2** or **3** (Table 1)[9,10] in DMSO or acetonitrile proceeded smoothly at 20 °C (Table 2). In some cases, the products were only identified by NMR spectroscopic analysis of the reaction mixture because they decomposed during workup. Phenyl isocyanate (**1a**) reacted with the carbanions **2c,d,i,k** (generated by deprotonation of the

Received: February 19, 2020

Table 1. Carbanions 2 and Enamines 3 Used for Determining the Electrophilicities of the Heteroallenes 1

Nucleophiles			N (s_N)[a]
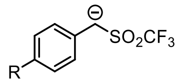	R = H	**2a**	18.67 (0.68) (DMSO)
	R = CF_3	**2b**	17.33 (0.74) (DMSO) 16.15 (0.99) (MeCN)[b]
	R = CN	**2c**	16.28 (0.75) (DMSO) 15.62 (0.99) (MeCN)[b]
	R = NO_2	**2d**	14.49 (0.86) (DMSO) 14.71 (1.05) (MeCN)[c]
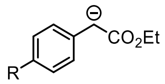	R = H	**2e**	27.54 (0.57) (DMSO)
	R = CN	**2f**	23.64 (0.65) (DMSO)
	R = NO_2	**2g**	20.00 (0.71) (DMSO)
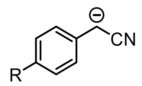	R = CN	**2h**	25.11 (0.54) (DMSO)
	R = NO_2	**2i**	19.67 (0.68) (DMSO) 20.10 (0.71) (MeCN)[b]
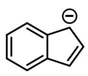 (K^+)		**2j**	24.16 (0.68) (DMSO)
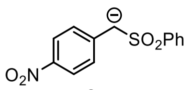		**2k**	18.50 (0.75) (DMSO) 19.90 (0.66) (MeCN)[b]
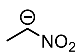		**2l**	21.54 (0.62) (DMSO)
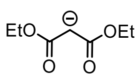		**2m**	20.22 (0.65) (DMSO)
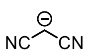		**2n**	19.36 (0.67) (DMSO)
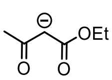		**2o**	18.82 (0.69) (DMSO)
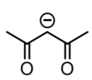		**2p**	17.64 (0.73) (DMSO)
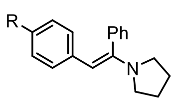	R = H	**3a**	11.66 (0.82) MeCN)
	R = NO_2	**3b**	10.42 (0.82) (MeCN)
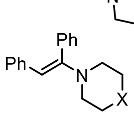	X = CH_2	**3c**	9.94 (0.86) (MeCN)
	X = O	**3d**	8.78 (0.83) (MeCN)

[a]With nucleophilicity parameters N and s_N from refs 8b and 9. [b]This work (Supporting Information). [c]Calculated from two rate constants in ref 9b.

conjugate acids **2**-H with KO*t*Bu) to form adducts. After aqueous workup the amides **4** were isolated (Table 2, entries 1–4).

While the reactions of phenyl isocyanate (**1a**) with isobutyraldehyde-derived enamines have been reported to give [2+2] cycloadducts,[11a] zwitterionic intermediates were characterized in reactions of *p*-tosyl isocyanate (**1b**) with *β*,*β*-dialkyl enamines.[11b] Nucleophilic addition of enamine **3a** to *p*-tosyl isocyanate (**1b**) and subsequent proton shift yielded a mixture of *E*-/*Z*-isomeric *β*-pyrrolidino-*α*,*β*-unsaturated enamides **4ba** (identified by two sets of pyrrolidino protons in the ^{1}H NMR spectrum, Supporting Information). As these enamides were difficult to separate and isolate, they were treated with 2% aqueous HCl to give the hydrolysis product **5ba**, which was isolated in 70% yield (Table 2, entry 5). Analogous reactions of tosyl isocyanate (**1b**) with other enamines have previously been reported.[12]

The adduct **4cn**$^-$Na$^+$, formed in the reaction of phenyl isothiocyanate (**1c**) with the malononitrile anion (**2n**), was identified by the NH resonance in the ^{1}H NMR spectrum (δ 8.89 ppm in d_6-DMSO) and the molecular anion peak in the high resolution mass spectrum (Table 2, entry 6). In analogy to the synthesis of ketene-*N*,*S*-acetals by Kirsch and co-workers,[13] iodomethane was used to methylate **4cn**$^-$Na$^+$ to yield **6cn** in 80% yield, which confirmed the structure of the initial adduct **4cn**$^-$ (Table 2, entry 9). The additions of carbanions **2o** and **2p** to the aryl isothiocyanates **1c** (Table 2, entries 7, 8) and **1d** (Table 2, entries 10–12) were carried out in analogy to entry 6 and analyzed by NMR spectroscopic methods without isolation of the products.

Ketene aminals were isolated in good yields when diphenyl carbodiimide (**1e**) was combined with various carbanions **2** (generated from their conjugate acids **2**-H and KO*t*Bu) in DMSO and subsequently treated with aqueous ammonium acetate solution (Table 2, entries 13–17). Potassium dithiocarboxylates were formed by the reactions of the pregenerated potassium salts **2f**,**g**-K with carbon disulfide (**1g**) in d_6-DMSO and identified by ^{1}H (**4gf**$^-$, **4gg**$^-$) and ^{13}C NMR (**4gf**$^-$) spectroscopy (Table 2, entries 18, 19). Treatment of CS_2 with 2-(4-nitrophenyl)acetonitrile (**2i**-H) and NaOH in d_6-DMSO gave an adduct, which tautomerized to give the enedithiolate anion **4gi**$^-$ (Table 2, entry 20). In order to match the situation of the kinetic investigations (use of excess CS_2) indenide (**2j**) was combined with 2 equiv of CS_2 (**1g**). The resulting mixture of two adducts was subsequently treated with iodomethane to give the corresponding methylation products **6gj** and **7gj** with 30% and 54% yield, respectively (Table 2, entry 21).

The indenide ion **2j** (generated in DMSO solution from **2j**-H and KO*t*Bu) reacted with solid CO_2 in DMSO to give 1*H*-indene-3-carboxylic acid (**4hj**) in 80% isolated yield after treatment with 2 M HCl (Table 2, entry 22, and Scheme 1). In contrast, several other carbanions did not yield a product when combined with CO_2 under similar conditions (Supporting Information, Chart S1). Only potassium fluorenide (generated in DMSO solution from fluorene and KO*t*Bu) gave trace amounts of fluorene-9-carboxylic acid, in accord with a study by Chiba, Miura, and co-workers who showed that carboxylation of CH acids with carbon dioxide (1 atm) required the presence of potassium carbonate and 18-crown-6 in the DMSO solutions.[14]

Kinetic Investigations. The kinetic investigations of the reactions of **1a**–**h** with the carbanions **2a**–**k** and the enamines **3** (reference nucleophiles listed in Table 1) were performed in DMSO or acetonitrile solution at 20 °C by following the disappearance of the UV/vis absorptions of the nucleophiles **2** and **3** under pseudo-first-order conditions ($[\mathbf{1}]_0/[\mathbf{2}(\text{or } \mathbf{3})]_0 > 7$). The first-order rate constants k_{obs} were obtained by least-squares fitting of the exponential function $A = A_0 \exp(-k_{obs}t) + C$ to the observed time-dependent absorbances of the reactants **2** or **3** (Figure 1a). The remaining absorbance at 344 nm during the reaction of **1a** with **2c** (Figure 1a) is due to the adduct **4ac**$^-$K$^+$, which was confirmed by measuring the UV/vis spectrum of a solution obtained by treatment of isolated **4ac** with KO*t*Bu. When the carbanions **2l**–**p** were used as reference nucleophiles, the kinetic investigations were performed by following the increase of the UV/vis absorbances of the products under pseudo-first-order conditions ($[\mathbf{2}]_0/[\mathbf{1}]_0 > 10$). The first-order rate constants k_{obs} were then obtained by least-squares

Table 2. Product Studies of Heteroallenes 1 with Carbanions 2 and Enamines 3

Entry	Heteroallenes		Nucleophiles	Reaction conditions	Products (Yield)[a]			
							R^1	R^2
1	Ph-N=C=O	**1a**	**2c**	(1) **2**-H, KO*t*Bu, MeCN, 20 °C (2) **1a**, 4 h (3) aq workup	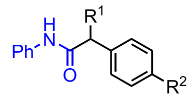	**4ac** (90%)	SO_2CF_3	CN
2		**1a**	**2d**			**4ad** (85%)	SO_2CF_3	NO_2
3		**1a**	**2i**			**4ai** (80%)	CN	NO_2
4		**1a**	**2k**			**4ak** (90%)	SO_2Ph	NO_2
5	Ts-N=C=O	**1b**	**3a**	CD_3CN, 20 °C, then 2% aq HCl	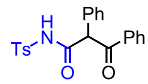	**5ba** (70%)		
							R^3	R^4
6	Ph-N=C=S	**1c**	**2n**	**2**-H, NaOH, d_6-DMSO, 2 h, 20 °C	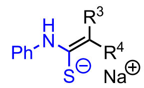	**4cn**$^-$ Na^+	CN	CN
7		**1c**	**2o**			**4co**$^-$ Na^+	COMe	CO_2Et
8		**1c**	**2p**			**4cp**$^-$ Na^+	COMe	COMe
9		**1c**	**2n**	(1) **2n**-H, NaOH, DMSO, 2 h, 20 °C (2) MeI, then aq workup	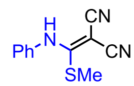	**6cn** (80%)		
							R^3	R^4
10	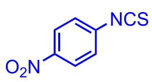	**1d**	**2n**	**2**-H, NaOH, d_6-DMSO 2 h, 20 °C	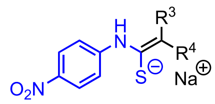	**4dn**$^-$ Na^+	CN	CN
11		**1d**	**2o**			**4do**$^-$ Na^+	COMe	CO_2Et
12		**1d**	**2p**			**4dp**$^-$ Na^+	COMe	COMe
							R^5	R^6
13	PhN=C=NPh	**1e**	**2a**	(1) **2**-H, KO*t*Bu, DMSO, 20 °C (2) **1e**, 4 h (3) aq workup	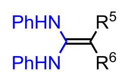	**4ea** (94%)	SO_2CF_3	Ph
14		**1e**	**2f**			**4ef** (74%)	CO_2Et	*p*-NC-C_6H_4
15		**1e**	**2h**			**4eh** (85%)	CN	*p*-NC-C_6H_4
16		**1e**	**2m**			**4em** (90%)	CO_2Et	CO_2Et
17		**1e**	**2o**			**4eo** (80%)	COMe	CO_2Et
18	S=C=S	**1g**	**2f**	**2**-K, d_6-DMSO, 20 °C, 2 h	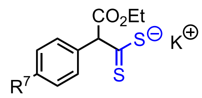	**4gf**$^-$ K^+	R^7 = CN	
19		**1g**	**2g**			**4gg**$^-$ K^+	NO_2	
20		**1g**	**2i**	**2i**-H, NaOH, d_6-DMSO 2 h, 20 °C	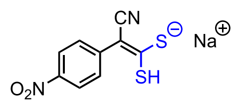	**4gi**$^-$ Na^+		
21		**1g**	**2j**	(1) **2j**-H, KO*t*Bu, DMSO, 20 °C (2) **1g**, 20 min (3) MeI, then aq workup	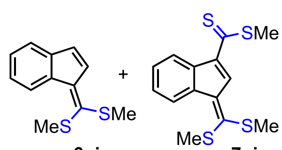 **6gj** **7gj**	**6gj** (30%) **7gj** (54%)		
22	O=C=O	**1h**	**2j**	(1) **2j**-H, KO*t*Bu, DMSO, 20 °C (2) **1h** (solid), 30 min (3) 2 M HCl	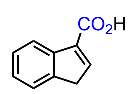	**4hj** (80%)		

[a]Yield of isolated product after chromatographic purification.

Scheme 1. Carboxylation of Indenide 2j

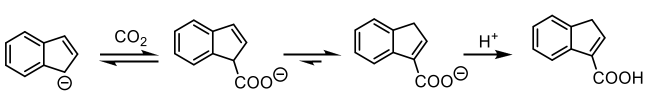

2j **(4hj')$^-$** **(4hj$^-$)** **4hj**

fitting of the exponential function $A = A_\infty [1 - \exp(-k_{obs}t)] + C$ to the observed time-dependent absorbances of the products.

The slopes of the linear correlations between k_{obs} and the variable concentrations of the excess components (Figure 1b) correspond to the second-order rate constants k_2^{exptl} listed in Table 3. Since the isocyanates **1a** and **1b** are not persistent in DMSO solution, kinetic experiments with these compounds were carried out in acetonitrile solution. The reactivity parameters N and s_N of carbanions **2b**, **2c**, **2d**, **2i**, and **2k** in acetonitrile have been determined in this work using our standard methods (Table 1 and section 5 in the Supporting Information). Reactivity parameters for these carbanions have previously been reported for DMSO solution (Table 1).

The preparation of DMSO solutions with different concentrations of carbon dioxide (**1h**) by diluting saturated solutions of CO_2 in DMSO and applying available data on the pressure-dependent solubility of CO_2 in DMSO[15] is explicitly described in the Supporting Information, section 7.

Figure 2 shows that the correlations of $(\log k_2)/s_N$ for the reactions of heteroallenes **1** with carbanions **2** and enamines **3** versus the corresponding nucleophilicity parameters N are linear with a slope of roughly 1 as required by eq 1. The reactions of these C_{sp}-centered electrophiles with enamines and carbanions thus follow the linear free-energy relationship eq 1 like the corresponding reactions of $C(sp^2)$-centered electrophiles.[8,9]

https://dx.doi.org/10.1021/jacs.0c01960
J. Am. Chem. Soc. XXXX, XXX, XXX−XXX

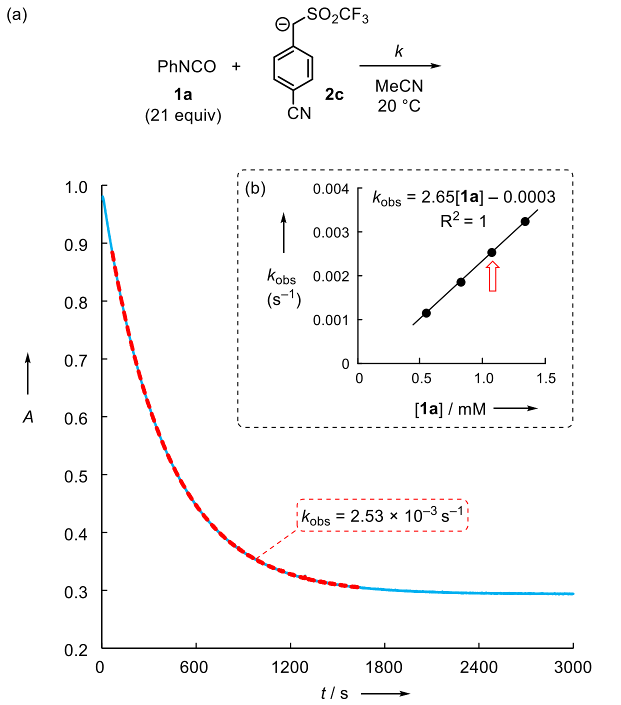

Figure 1. (a) Monoexponential decay of the absorbance A (at 344 nm) of **2c** during the reaction of **1a** (1.07×10^{-3} M) with **2c** (5.00×10^{-5} M) in acetonitrile at 20 °C. (b) Plot of k_{obs} for the reaction of **1a** with **2c** versus the concentration of **1a**.

Least-squares optimization [minimization of $\Delta^2 = \sum(\log k_2^{\text{exptl}} - \log k_2^{\text{eq 1}})^2] = \sum(\log k_2^{\text{exptl}} - s_N(N + E))^2]$ of the rate constants of the reactions of **1a**−**e** and **1g** with carbanions **2** and enamines **3** gave the electrophilicity parameters E for the heteroallenes **1** in the second column of Table 3. Since the kinetics of nucleophilic additions to CO_2 could only be measured for one carbanion, the listed E value for CO_2 could not be confirmed independently. Due to the low intrinsic barriers, the reactions of CO_2 with carbanions of higher basicity can be expected to approach diffusion control, and therefore, cannot be used to derive a more reliable electrophilicity parameter E for CO_2.

Quantum Chemical Calculations. As illustrated in Scheme 2, attack of a carbanion at the central carbon of heteroallenes initially yields the heteroallyl anion **IA**, which may tautomerize to **TA** with an equilibrium constant depending predominantly on the nature of R, Y, R^1, and R^2, whereas X and R′ play a minor role (X-R′ is part of the heteroallyl anion system in **IA** *and* **TA**).

Activation and reaction Gibbs energies for the reactions of the symmetrical (CS_2, CO_2) and unsymmetrical (**1a**, **1c**) heteroallenes with the carbanion **2n** were calculated at the IEFPCM-(DMSO)/B3LYP-D3/6-311+G(d,p) level of theory.[16a−c] As illustrated in Figure 3, the nucleophilic attack at CO_2 is faster, but thermodynamically less favorable than attack at CS_2. Proton shift converts the initially formed adducts **IA** into the tautomers **TA**, which are 22 (**4hn**$^-$) and 37 kJ mol^{-1} (**4gn**$^-$) more stable.

Figure 4 shows that the formation of the new CC bond is further advanced in the transition state of the reaction with CO_2 (2.17 Å) than in the reaction with CS_2 (2.25 Å). In other words, the reaction with CO_2 proceeds via a later transition state.

Distortion interaction analysis[17] shows that deformation of the nucleophile $(NC)_2CH^-$ (**2n**) requires very little energy (Figure 5, left), in line with the well-known flat energy surface for pyramidalization of the malononitrile anion, which accounts for the low intrinsic barriers for its reactions with Michael acceptors.[18] Thus, the major contribution to the distortion energy comes from the heteroallene. Figure 5 (left) shows that before reaching the transition state, distortion of the S=C=S fragment generally requires more energy than distortion of the O=C=O part. Since the interaction energy is similar for the reactions with CO_2 and CS_2 (Figure 5, right, green lines), the reaction with CS_2 proceeds via an earlier, higher energy transition state than the reaction with CO_2 (Figure 5, right, black lines).

Due to the lower symmetry, the situation is more complex for the reactions with phenyl isocyanate (**1a**) and phenyl isothiocyanate (**1c**). As illustrated in Figure 6 for the reaction of the malononitrile anion (**2n**) with **1a**, variation of the dihedral angle C_{Ar}−N−C−C_{Nu} at a constrained length of the new CC bond (2.30 Å) results in two discrete minima at 180° and 25°, which indicate that the nucleophile **2n** does not attack from top or bottom of the molecular plane, which would be expected if the reaction would be controlled by interaction with LUMO-(**1a**), but from two directions (*anti* and *syn*) in or close to the molecular plane of **1a**.

Intrinsic reaction coordinate (IRC) calculations show that the *anti* attack proceeds perfectly in the molecular plane and is controlled by interaction with π^*(CO), i.e., LUMO+2 of phenyl isocyanate (**1a**). In the corresponding transition state **TS(B)**, depicted in Figure 7, all atoms of phenyl isocyanate and the methine carbon of the attacking carbanion are perfectly coplanar.

The alternative trajectory (*syn* attack) is controlled by interaction of the HOMO(**2n**) with both, LUMO and LUMO+2, of **1a** and begins with a gauche approach of **2n** at **1a** (dihedral angle C_{Ar}−N−C−C_{Nu} is 44° at a distance of 3.24 Å). As the nucleophile gets closer, it moves more and more into the molecular plane of **1a** as indicated by the dihedral angle of 25° at 2.30 Å distance (Figure 6) and of 15.5° at the transition state **TS(A)** in Figure 7. The different views of the transition states in Figure 7 furthermore show that in the *syn* transition state **TS(A)**, the phenyl ring is strongly twisted toward the plane of the developing heteroallyl anion (C_{Ar}−C_{Ar}−N−C = 127°) and thus gives up conjugation.

The energetics of the entire reaction cascades are shown in Figure 8a. The larger lobe of LUMO+2 on the *syn* side and the additional interaction with LUMO can explain why the *syn* pathway proceeds via a lower barrier than the *anti* pathway (57.8 vs 70.9 kJ mol^{-1}). In the initially formed adducts (**IA**), the relative energies are inverted, however, and the product arising from *anti* attack, **IA(B)**, is more stable than **IA(A)** by 10 kJ mol^{-1}. Both initially formed adducts **IA** undergo a proton transfer to the more stable tautomers (*E*)-**TA** and (*Z*)-**TA**. Rapid rotation around the C−N single bond transforms (*E*)-**TA** into (*Z*)-**TA**, the most stable reaction product. The tautomerization step reflects the fact that malononitrile is a stronger Brønsted acid than aniline.

A similar pattern of relative Gibbs energies of transition states and adducts **IA** and **TA** was calculated for the reaction of **2n** with the sulfur analog **1c** (Figure 8b).

Figure 9 illustrates the distortion interaction analysis for the reaction of malononitrile anion (**2n**) with phenyl isocyanate (**1a**). As described above for the reactions with CO_2 and CS_2 (Figure 5), the distortion energies of the anion **2n** are very small for both reaction pathways (Figure 9, left) and the distortion

https://dx.doi.org/10.1021/jacs.0c01960
J. Am. Chem. Soc. XXXX, XXX, XXX−XXX

Table 3. Experimental (k_2^{exptl}) and Calculated ($k_2^{\text{eq 1}}$) Second-Order Rate Constants for the Reactions of Heteroallenes 1 with Nucleophiles 2 and 3 at 20 °C

Heteroallenes	Electrophilicity E	Nucleophiles	k_2^{exptl} (M^{-1} s^{-1})	$k_2^{\text{eq 1}}$ [a] (M^{-1} s^{-1})	$k_2^{\text{exptl}}/k_2^{\text{eq 1}}$
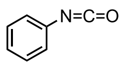 **1a**	−15.38 (in MeCN)	**2b**	(2.49 ± 0.08) × 10^1	5.78	4.3
		2c	(2.65 ± 0.02)	1.73	1.5
		2d	(3.29 ± 0.03) × 10^{-1}	1.98 × 10^{-1}	1.7
		2i	(2.35 ± 0.16) × 10^2	2.24 × 10^3	0.10
		2k	(2.94 ± 0.05) × 10^2	9.62 × 10^2	0.31
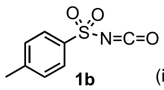 **1b**	−7.69 (in MeCN)	**3a**	(2.07 ± 0.07) × 10^3	1.80 × 10^3	1.2
		3b	(1.80 ± 0.06) × 10^2	1.73 × 10^2	1.0
		3c	(7.56 ± 0.43) × 10^1	8.61 × 10^1	0.88
		3d	(7.96 ± 0.83)	8.03	0.99
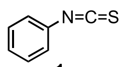 **1c**	−18.15 (in DMSO)	**2a**	(2.03 ± 0.08)	2.26	0.90
		2l	(5.28 ± 0.18) × 10^1	1.26 × 10^2	0.42
		2n	(2.69 ± 0.04) × 10^1	6.47	4.2
		2o	(1.15 ± 0.01)	2.90	0.40
		2p	(6.45 ± 0.28) × 10^{-1}	4.24 × 10^{-1}	1.5
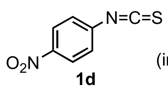 **1d**	−15.89 (in DMSO)	**2c**	(2.47 ± 0.06)	1.96	1.3
		2m	(2.72 ± 0.04) × 10^2	6.52 × 10^2	0.42
		2n	(1.24 ± 0.02) × 10^3	2.11 × 10^2	5.9
		2o	(9.08 ± 0.14) × 10^1	1.05 × 10^2	0.86
		2p	(7.58 ± 1.12)	1.89 × 10^1	0.40
PhN=C=NPh **1e**	−20.14 (in DMSO)	**2a**	(2.80 ± 0.17) × 10^{-1}	1.00 × 10^{-1}	2.8
		2f	(1.42 ± 0.18) × 10^2	1.88 × 10^2	0.75
		2h	(1.69 ± 0.05) × 10^2	4.83 × 10^2	0.35
		2m	(5.96 ± 0.39) × 10^{-1}	1.13	0.53
		2o	(2.41 ± 0.18) × 10^{-1}	1.23 × 10^{-1}	2.0
CyN=C=NCy **1f**	(−30)[b] (in DMSO)	**2e**	very slow[c]		
S=C=S **1g**	−17.70 (in DMSO)	**2a**	(1.00 ± 0.02) × 10^1	4.57	2.2
		2b	(4.19 ± 0.26) × 10^{-1}	5.32 × 10^{-1}	0.79
		2f	(1.78 ± 0.21) × 10^3	7.26 × 10^3	0.25
		2g	(2.19 ± 0.04) × 10^1	4.30 × 10^1	0.51
		2i	(2.60 ± 0.07) × 10^1	2.19 × 10^1	1.2
		2j	(9.76 ± 0.96) × 10^4	2.47 × 10^4	4.0
O=C=O **1h**	≈ −16.3 (in DMSO)	**2j**	(2.09 ± 0.07) × 10^5		

[a]Calculated by using eq 1, N and s_N from Table 1, and E from this table. [b]E value is derived by quantum chemical calculation. [c]Too slow to be measured.

energy of the isocyanate **1a** is much greater for the *anti* attack than for the *syn* attack.

The right part of Figure 9 shows that the interaction energies (green) for the two pathways are almost identical in the first part of the reaction coordinate (C−C > 2 Å). For that reason, the transition state of the *anti* attack **TS(B)** is reached earlier (C−C = 2.30 Å) than **TS(A)** of the *syn* attack (C−C = 2.17 Å). The smaller activation energy for the *syn* attack is thus due to the fact that the distortion energies at the transition states of both pathways are almost the same, while the interaction energy is much larger at the later transition state **TS(A)** of the *syn* attack.

Figure 10 compares the geometry of phenyl isocyanate with those of the distorted phenyl isocyanate fragments in the two reaction pathways. At a distance of 2.45 Å between the two reaction centers, the O−C−N angle is slightly more distorted in the *syn* pathway than in the *anti* pathway. The larger distortion energy of the *anti* attack must, therefore, be due to the distortion of the C−N−C_{Ar} angle, which is strongly reduced from 141.9° to 121.1° in the *anti* pathway and only to 136.4° in the *syn* pathway.

Comparison of the origin of the different reactivities of phenyl isocyanate (**1a**) and phenyl isothiocyanate (**1c**) shows analogous phenomena as the comparison of CO_2 and CS_2. Figure 8 already indicates that nucleophilic attack at the sulfur derivative **1c** is more exergonic (for the formation of **IA**) than attack at the oxygen analogue **1a**. Figure 8 also shows that the kinetic preference of nucleophilic attack at phenyl isocyanate (**1a**) compared to phenyl isothiocyanate (**1c**) (18.2 kJ mol^{-1} for the *syn* path) is slightly smaller than the kinetic preference of CO_2 over CS_2. Figure 11 reveals the reason: It is again the larger distortion energy of the sulfur-containing compound **1c** which accounts for its lower reactivity compared to the oxygen-containing analog **1a**.

Consistency of Data: Comparison of Calculated and Experimental Activation Energies. As illustrated in Figure 12a, the DFT-calculated Gibbs activation energies $\Delta G^{\ddagger}_{\text{calcd}}$ for the reactions of the heteroallenes **1a**−**h** with the nucleophiles **2a** and **2n** correlate with high quality, confirming the consistency of the calculated numbers. On the other hand, the analogous

https://dx.doi.org/10.1021/jacs.0c01960
J. Am. Chem. Soc. XXXX, XXX, XXX−XXX

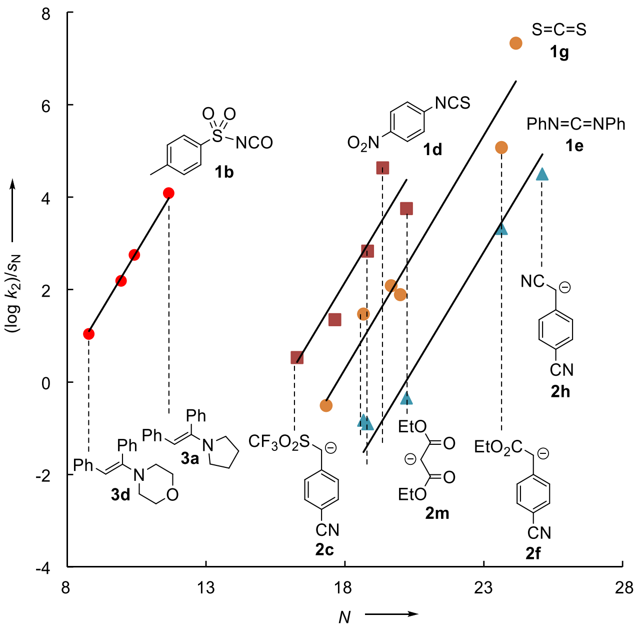

Figure 2. Plots of $(\log k_2)/s_N$ vs N for the reactions of heteroallenes **1** with carbanions **2** and enamines **3** in DMSO or acetonitrile at 20 °C (the slope of the depicted correlation lines is enforced to 1). For the sake of clarity, the correlation lines for **1a** and **1c** are shown only in the Supporting Information (Figure S13).

Scheme 2. Mechanism of the Reactions of Heteroallenes with Carbanions

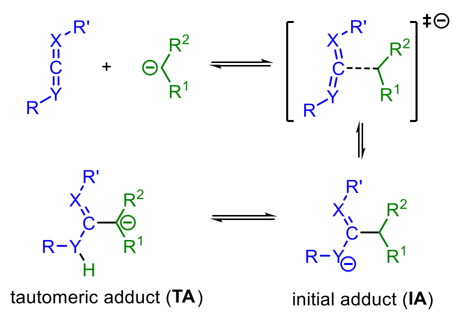

correlations between the barriers for the indenide ion (**2j**) and **2n** (Figure 12b) or **2a** (Supporting Information, Figure S26C) show a higher scatter, indicating that the indenide ion (**2j**) behaves differently from the other nucleophiles and may, therefore, not be a suitable reference nucleophile for the parametrization of electrophilic reactivities. This insight is unfortunate as **2j** was the only nucleophile which we could use for determining the electrophilicity of CO_2.

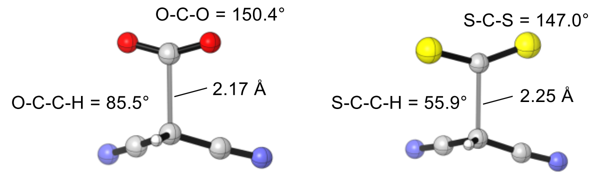

Figure 4. Geometries of the transition states[16d] for the reactions of **1g** and **1h** with **2n** at the IEFPCM(DMSO)/B3LYP-D3/6-311+G(d,p) level of theory.

Table 4 shows that all quantum chemically calculated Gibbs activation energies $\Delta G^{\ddagger}_{\text{calcd}}$ agree with the directly measured values (printed in parentheses in Table 4) within 13 kJ mol^{-1}. If one excludes the reaction of carbanion **2a** with CO_2 (**1h**), the standard deviation between experimental $\Delta G^{\ddagger}$ (i.e., $\Delta G^{\ddagger}_{\text{exptl}}$ directly measured or derived from eq 1) and DFT calculated Gibbs activation energies $\Delta G^{\ddagger}_{\text{calcd}}$ is ±12 kJ mol^{-1}.

The Gibbs activation energies $\Delta G^{\ddagger}_{\text{exptl}}$ for the reactions of the heteroallenes **1** with **2n** derived by eq 1 using N and s_N from Table 1 and E from Table 3 correlate well with the DFT calculated values (exception **1h**, Figure 13a). If the insecure entry for CO_2 (**1h**) is neglected, a correlation between experiment and theory with a slope of 1.02 is obtained. The intercept of this correlation implies that the experimental activation energies are in average 6 kJ mol^{-1} smaller than the theoretical values. An analogous correlation for the reactions of carbanion **2a** with the heteroallenes **1** is of slightly lower quality (R^2 = 0.92, Supporting Information, Figure S29A). As a consequence of these linear correlations, there is also a linear correlation between the empirical electrophilicity parameters E of the heteroallenes **1** with the calculated Gibbs activation energies $\Delta G^{\ddagger}_{\text{calcd}}$ for their reactions with carbanion **2n** (Figure 13b). From the correlation in Figure 13b one would expect an electrophilicity parameter $E = -11.4$ for CO_2.

What is the reason for the strikingly unique position of CO_2 in these correlations? We assume that the origin for the deviation of CO_2 in the correlations in Figure 13 is due to the fact that the indenide ion **2j**, which was used as reference for the calculation

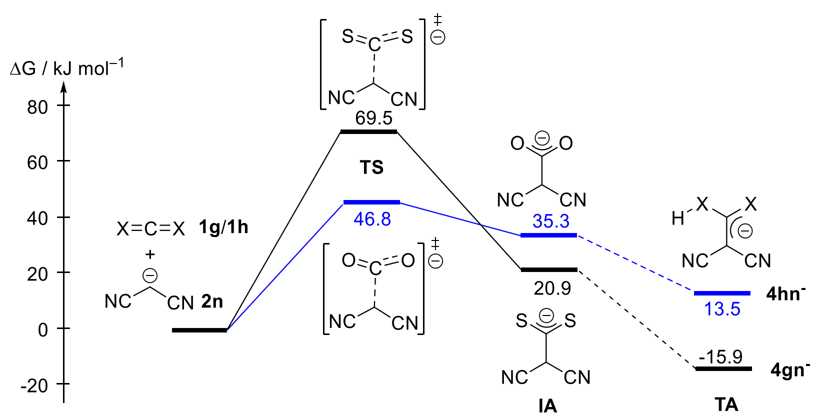

Figure 3. Gibbs energy profiles for the reactions of malononitrile anion **2n** with CS_2 (**1g**, black pathway) and CO_2 (**1h**, blue pathway) at the IEFPCM(DMSO)/B3LYP-D3/6-311+G(d,p) level of theory.

https://dx.doi.org/10.1021/jacs.0c01960
J. Am. Chem. Soc. XXXX, XXX, XXX−XXX

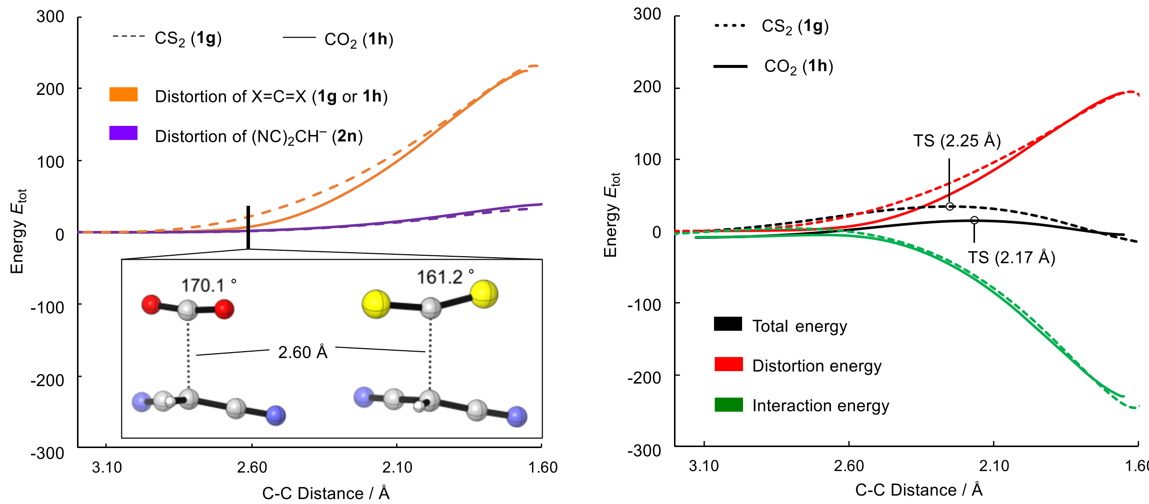

Figure 5. Distortion interaction analysis of the transition states for the reaction of **2n** with the heteroallenes **1g** and **1h** calculated at the IEFPCM(DMSO)/B3LYP-D3/6-311+G(d,p) level of theory (electronic energies E_{tot} in kJ mol^{-1}). Inset: Geometries at a C−C distance of 2.60 Å.[16d]

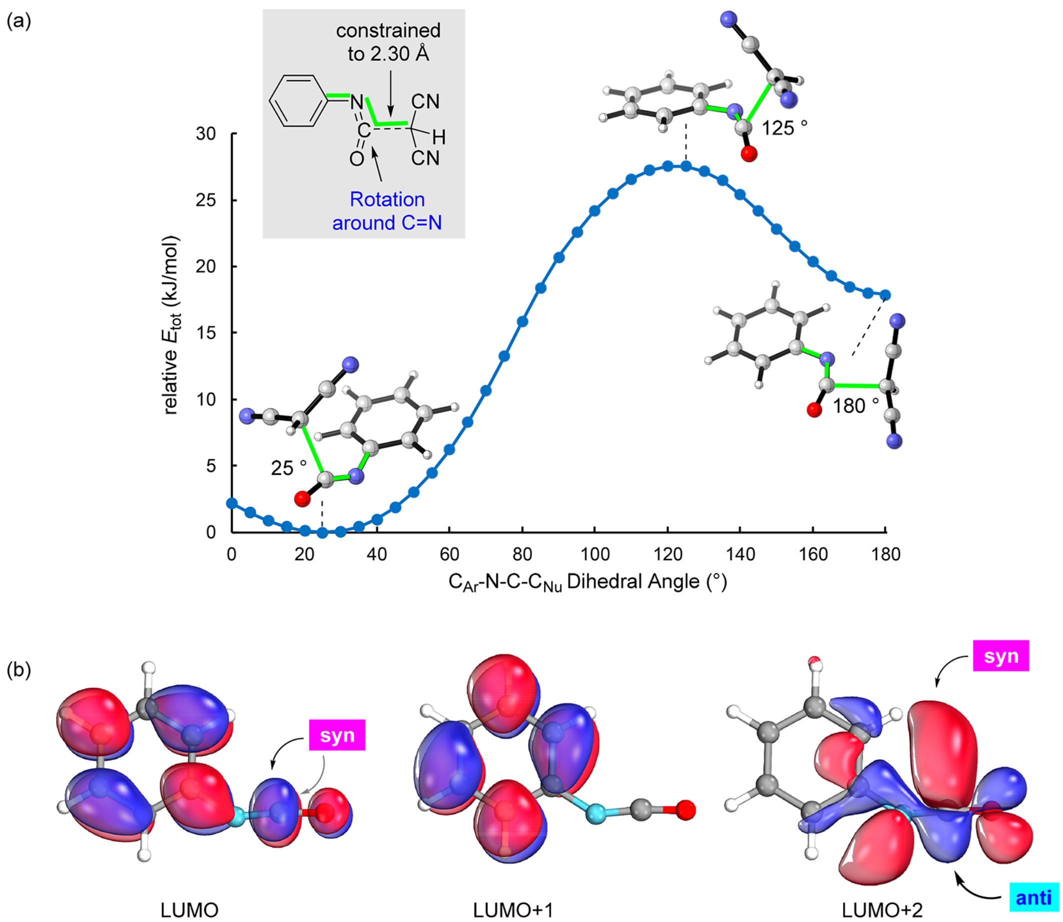

Figure 6. (a) Dependence of E_{tot} for a complex of PhNCO (**1a**) with the carbanion **2n** on the dihedral angle C_{Ar}−N−C−C_{Nu} at a constrained length (2.30 Å) of the new CC bond (at the IEFPCM(DMSO)/B3LYP-D3/6-311+G(d,p) level of theory). (b) Unoccupied frontier orbitals of phenyl isocyanate (**1a**)[16e] calculated at the IEFPCM(DMSO)/B3LYP-D3/Def2TZVP//IEFPCM(DMSO)/B3LYP-D3/6-311+G(d,p) level of theory.

of $E(CO_2)$, is not a well-behaved nucleophile as shown above (see discussion of Figure 12b). A further examination of this hypothesis was not possible because of our failure to determine kinetics of the reaction of CO_2 with other carbanions.

Rate Equilibrium Relationships. Relationships between rate constants and the corresponding Gibbs reaction energies are among the most important tools for elucidating the origin of activation barriers. Brønsted correlations, Bell−Evans−Polanyi relationships, and Leffler−Hammond analyses are the best known treatments.[19] Since in most reactions investigated in this work, the initially formed adducts **IA** undergo fast proton shifts with formation of **TA** (Scheme 2), it is very difficult, if not impossible, to determine the reaction energy for the formation of **IA** experimentally. For that reason, we calculated the Gibbs

https://dx.doi.org/10.1021/jacs.0c01960
J. Am. Chem. Soc. XXXX, XXX, XXX−XXX

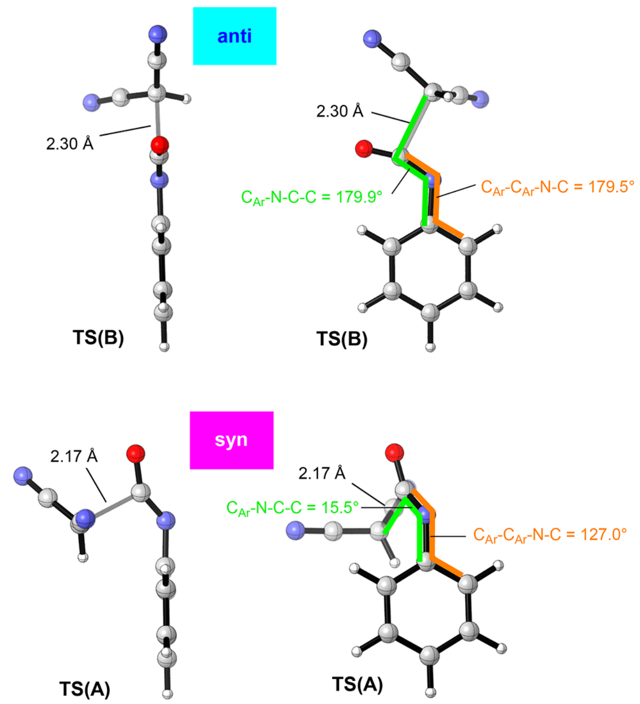

Figure 7. Geometries of the *syn* and *anti* transition states[16d] for the reaction of PhNCO (**1a**) with the carbanion **2n** at the IEFPCM-(DMSO)/B3LYP-D3/6-311+G(d,p) level of theory.

reaction energies Δ_rG^0 for the reactions of heteroallenes **1a−h** with the carbanions **2a**, **2n**, and **2j** by DFT methods (Table 5).

The linear correlation between the calculated Gibbs energies $\Delta_rG^0_{calcd}$(**IA**) for the reaction of **1** with **2a** versus the corresponding Gibbs energies for the reaction of **1** with **2n** shows the consistency of the calculated $\Delta_rG^0_{calcd}$ for reactions of **1** with different nucleophiles (Figure 14). The analogous correlation for **2j** vs **2n** is depicted in the Supporting Information (Figure S23B, R^2 = 0.975). Figure 15 shows that the quantum chemically calculated activation barriers $\Delta G^{\ddagger}_{calcd}$ for the reactions of the carbanions **2a**, **2n**, and **2j** with the heteroallenes **1b−g** correlate linearly with the corresponding Gibbs reaction energies Δ_rG^0(**IA**). The slopes of these Leffler−Hammond-type correlations ($0.49 \leq \alpha \leq 0.63$) indicate that approximately half of the changes of the Gibbs reaction energies are reflected by the Gibbs activation energies. However, phenyl isocyanate (**1a**) and CO_2 (**1h**) are significantly below the correlation lines in all three correlations, indicating that **1a** and **1h** react with significantly lower intrinsic barriers than the other heteroallenes.

What makes the heteroallenes **1a** and **1h** special? Since the quantum-chemically calculated $\Delta G^{\ddagger}$ values in Figure 15 do not suffer from the uncertainty of the experimental value for CO_2, we assume that it is the presence of a C═O double bond. Earlier work has already shown that carbonyl groups react much faster with nucleophiles than electron-deficient CC double bonds of equal Lewis acidity (expressed by methyl anion affinities, i.e., the negative of the Gibbs reaction energies, Figure 16).[20b] The fact that *p*-tosyl isocyanate (**1b**), which also bears a carbonyl group, does not show deviating behavior in Figure 15 may be due to the fact that the tosylamido group is a stronger electron-accepting group than the carbonyl group with the consequence that charge delocalization into the carbonyl group is less important than in the reactions with phenyl isocyanate (**1a**) and carbon dioxide (**1h**).

Previous studies revealed good correlations between the experimental electrophilicity parameters *E* of Michael acceptors and ketones and the quantum chemically calculated methyl anion affinities (MAAs), which are defined analogously as the MAAs of heteroallenes in eq 2.[20] The two classes of compounds

followed separate correlations, however, and ketones (C═O) were found to be much more electrophilic than Michael acceptors (C═C) of comparable MAA (Figure 16).[20b]

In view of the large structural variety of the heteroallenes under investigation it is, therefore, not surprising that there is no good correlation between the electrophilicities *E* of the heteroallenes **1** and their MAAs. It is noteworthy, however, that heteroallenes are much less electrophilic than structurally related ketones and Michael acceptors of comparable MAA, indicating that cumulated double bonds react over higher intrinsic barriers than ordinary double bonds.

Structure−Reactivity Relationships. After establishing the agreement between experimental and quantum chemically derived Gibbs activation energies for nucleophilic additions to heteroallenes **1**, let us now consider the influence of structural changes in **1** on electrophilicity and Lewis acidity (Figure 17). The excellent correlation between Gibbs activation energies for the reactions of the heteroallenes **1** with **2a** and **2n** (Figure 12a) implies that reactivities toward either of these carbanions can be used for this comparison.

The values of $\Delta_rG^0_{calcd}$(**IA**) in Figure 17b indicate that tosyl isocyanate (**1b**) is the only heteroallene in this series, which yields the initial adduct **IA** with the malononitrile anion **2n** by an exergonic process. The other reactions of **2n** proceed with endergonic formation of the initial adducts **IA**, which subsequently undergo a proton shift to give the thermodynamically more stable tautomers **TA** (Tables 2 and 5). Only the reaction of **2n** with CO_2 remains endergonic even after tautomerization (Table 5).

Diphenylcarbodiimide (**1e**), marked by the blue background color in Figure 17, is the least electrophilic compound of this series, for which calculated and experimental activation energies are available. Replacement of the phenyl groups by cyclohexyl (**1e** → **1f**) increases the Gibbs activation energy of the reaction with **2n** by 39 kJ mol^{-1}. Figure 12a implies that similar effects can be expected for reactions of **1** with other nucleophiles. With an estimated electrophilicity $E \approx -30$ (from $\Delta G^{\ddagger}_{calcd}$ in Table 4 using the correlation in Figure 13b) the reactivity of *N,N′*-dicyclohexylcarbodiimide (DCC, **1f**) is so low that we did not find any reference nucleophile suitable for kinetic measurements. This observation is in line with the generally accepted reaction mechanism for DCC-mediated peptide-forming reactions, which proceed via initial protonation of DCC to generate a more electrophilic species that subsequently reacts with carboxylate anions.[21]

Successive replacement of the PhN groups of carbodiimide **1e** by oxygen to give phenyl isocyanate **1a** and carbon dioxide **1h**, reduces the activation Gibbs energies by 17 and 11 kJ mol^{-1}, respectively. The analogous substitution of PhN by sulfur (**1e** → **1c** → **1g**) has no or very little influence on reaction rates (Figure 17a). The differences between the O- and S-series are due to different intrinsic barriers in the two series since Figure 17b shows that in the first series (replacement of NPh by O, **1e** → **1a**

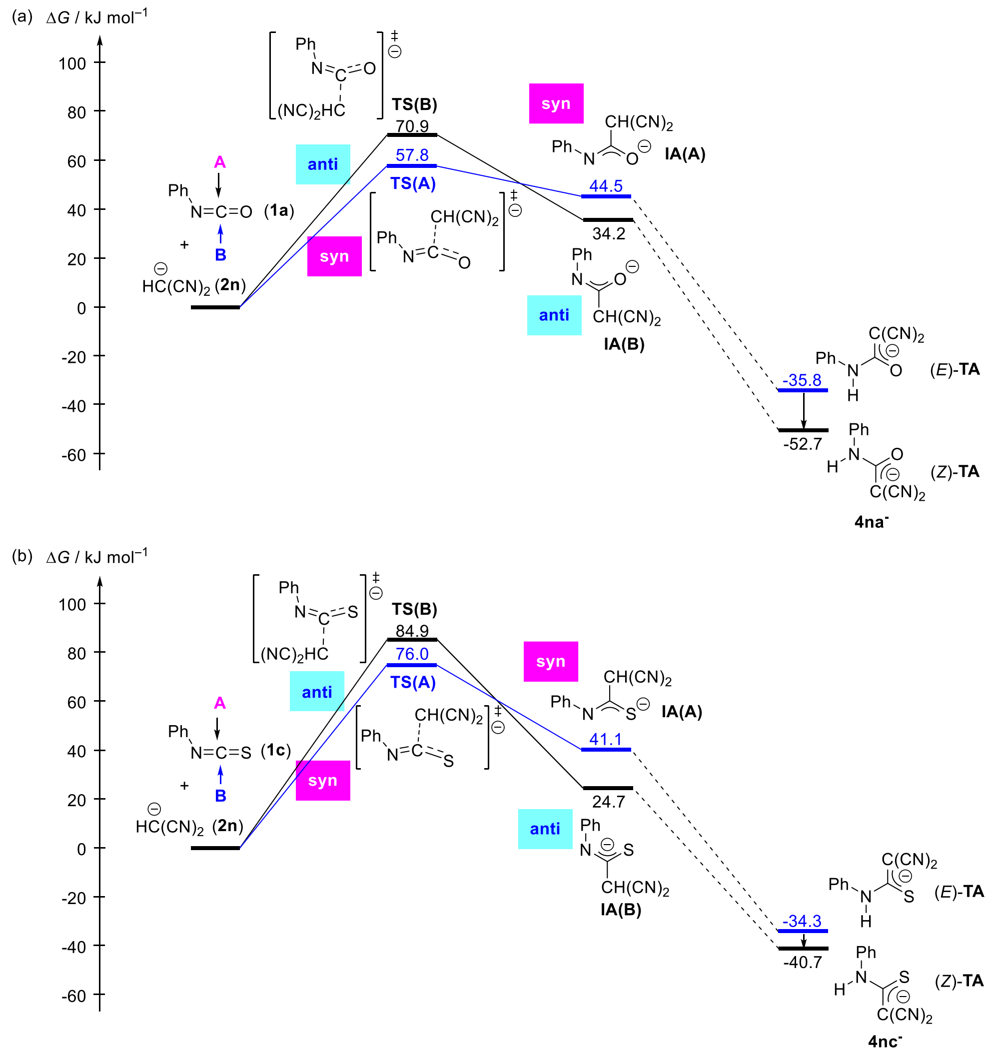

Figure 8. Energy profiles (ΔG, in kJ mol^{-1}) for the *syn* and *anti* pathways of the reactions of the malononitrile anion (**2n**) with **1a** (a) and **1c** (b) at the IEFPCM(DMSO)/B3LYP-D3/6-311+G(d,p) level of theory. Energies refer to the energetically lowest lying conformer for the depicted mode of attack.

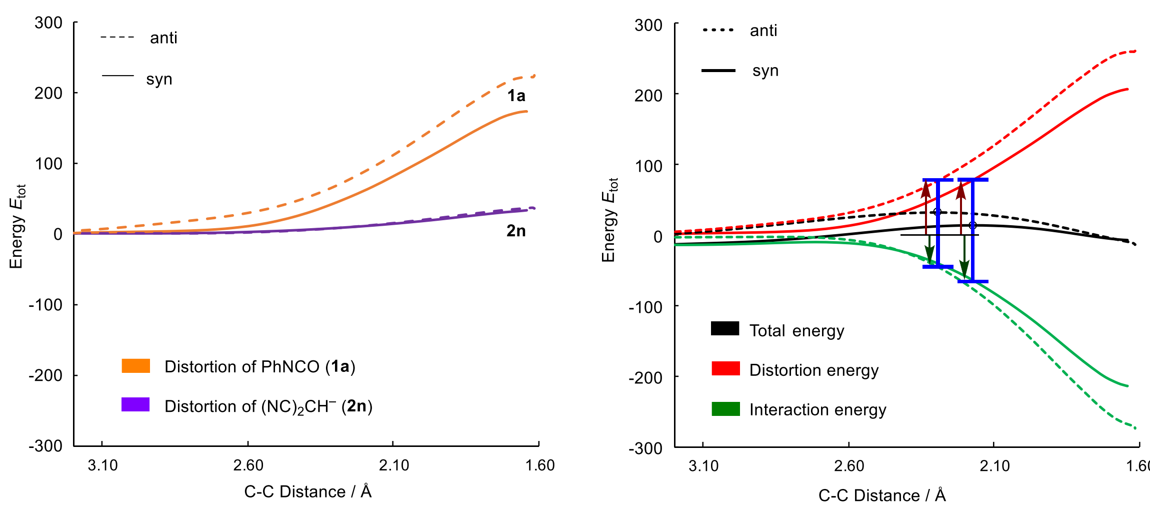

Figure 9. Distortion interaction analysis on the IRC pathways for the *syn* and *anti* pathways of the reaction of the malononitrile anion (**2n**) with phenyl isocyanate (**1a**).

→ **1h**) the Gibbs reaction energy decreases only marginally, while replacement of NPh by S (**1e** → **1c** → **1g**) reduces $\Delta_r G^0_{calcd}$(**IA**) by 15 and 4 kJ mol^{-1}. PhNCO (**1a**) is thus a significantly stronger electrophile than PhNCS (**1c**) while the

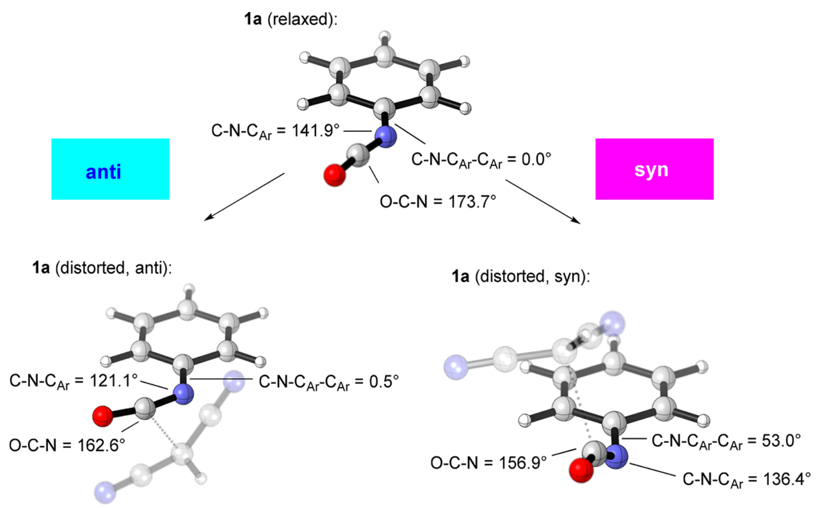

Figure 10. Comparison of the geometries of the relaxed and distorted phenyl isocyanate fragments at a C−C distance of 2.45 Å.[16d]

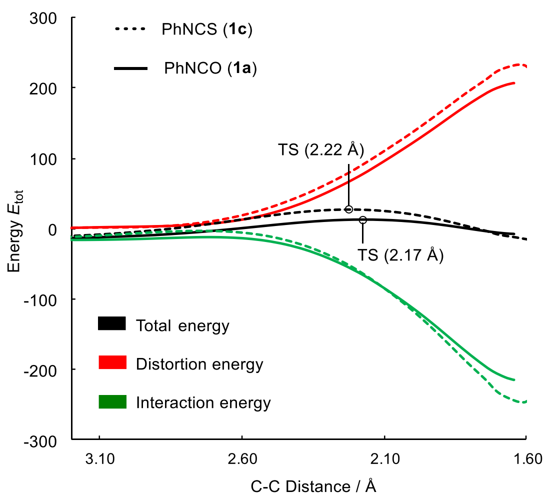

Figure 11. Distortion interaction analysis of the kinetically favored *syn* pathways of the reactions of **2n** with phenyl isocyanate (**1a**) and phenyl isothiocyanate (**1c**) calculated at the IEFPCM(DMSO)/B3LYP-D3/6-311+G(d,p) level of theory.

relative thermodynamic driving forces are vice versa, i.e., the stronger electrophile is the weaker Lewis acid. An analogous relationship is found for CS_2 and CO_2: Nucleophilic additions to CO_2 proceed faster, but have lower thermodynamic driving forces.

Electrophilicity Parameters *E* as Ordering Principle for Heteroallene Reactivities. The electrophilicity parameters *E* of the carbonyl derivatives and Michael acceptors shown in the left part of Figure 18 have previously been derived from the kinetics of their reactions with C-centered nucleophiles, like those for the heteroallenes in this work (Table 3). Figure 18 illustrates that tosyl isocyanate (**1b**), the most reactive heteroallene of this series, has an electrophilicity comparable to that of 1,1-bisphenylsulfonyl-ethylene, the most reactive Michael acceptor we have parametrized so far. Phenyl isocyanate (**1a**), which is 8 orders of magnitude less reactive than **1b** (toward nucleophiles with s_N = 1), has an electrophilicity comparable to that of *trans*-1,2-dicyanoethylene, and the electrophilicity of diphenylcarbodiimide (**1e**) is slightly lower than that of diethyl maleate. The calculated electrophilicity of

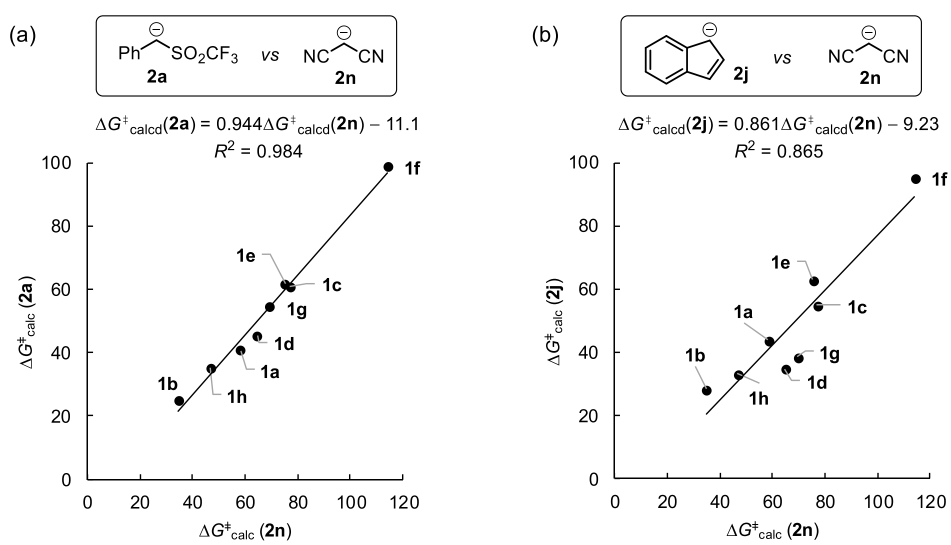

Figure 12. Correlation between Gibbs activation energies $\Delta G^\ddagger_{calcd}$ (kJ mol^{-1}) for the reactions of heteroallenes **1a**−**h** with different carbanions calculated at the IEFPCM(DMSO)/B3LYP-D3/6-311+G(d,p) level of theory.

https://dx.doi.org/10.1021/jacs.0c01960
J. Am. Chem. Soc. XXXX, XXX, XXX−XXX

Table 4. Experimental and Quantum Chemically Calculated Gibbs Energies of Activation (kJ mol^{-1}) for the Reactions of Heteroallenes 1 with Carbanions 2a, 2n, and 2j (in DMSO)

1	E	2a		2n		2j	
		$\Delta G^{\ddagger}_{calcd}$ [a]	$\Delta G^{\ddagger}_{exptl}$ [b]	$\Delta G^{\ddagger}_{calcd}$ [a]	$\Delta G^{\ddagger}_{exptl}$ [b]	$\Delta G^{\ddagger}_{calcd}$ [a]	$\Delta G^{\ddagger}_{exptl}$ [b]
PhNCO (**1a**)	−15.38	41	59[c]	58	57[c]	44	38[c]
TsNCO (**1b**)	−7.69	25	30[c]	35	28[c]	28	(9)[d]
PhNCS (**1c**)	−18.15	61	70 (70)[e]	77	67 (64)[e]	55	49
p-$NO_2C_6H_4NCS$ (**1d**)	−15.89	45	61	65	59 (54)[e]	35	40
PhNCNPh (**1e**)	−20.14	62	77 (75)[e]	75	75	63	56
CyNCNCy (**1f**)	-	99	-	114	-	95	-
CS_2 (**1g**)	−17.70	54	68 (66)[e]	70	65	39	47 (44)[e]
CO_2 (**1h**)	≈−16.3	35	63	47	60	33	42 (42)[e]

[a]Calculated at the IEFPCM(DMSO)/B3LYP-D3/6-311+G(d,p) level of theory for 25 °C (Supporting Information). [b]Derived from the electrophilicity E and the nucleophile-specific parameters N and s_N based on eq 1 for 20 °C. [c]In acetonitrile. [d]Diffusion-controlled reaction. [e]Directly measured at 20 °C.

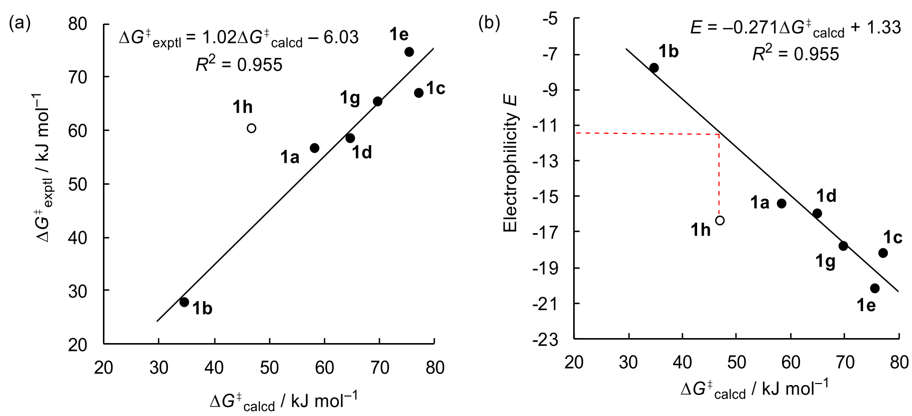

Figure 13. (a) Correlation of experimental Gibbs activation energies $\Delta G^{\ddagger}_{exptl}$ for the reactions of **2n** with **1a-h** (from eq 1 using N and s_N from Table 1 and E from Table 3; data for CO_2 not used for the correlation) against $\Delta G^{\ddagger}_{calcd}$ calculated at the IEFPCM(DMSO)/B3LYP-D3/6-311+G(d,p) level of theory. (b) Analogous correlation between electrophilicities E and the calculated Gibbs activation energies $\Delta G^{\ddagger}_{calcd}$ for the reactions of **1** with **2n**.

dicyclohexylcarbodiimide (**1f**) is significantly lower than that of all Michael acceptors we have parametrized so far.

It should be noted, however, that this comparison refers explicitly to kinetics. From the relative MAAs depicted in Figure 16, one can derive that nucleophilic additions to heteroallenes **1** without C═O group are more exergonic than the corresponding reactions with ketones and Michael acceptors of similar electrophilicity, which can be explained by release of strain of the cumulated double bonds. Though we were not able to derive a reliable value for the electrophilicity of CO_2, Figure 18 shows that it is comparable to that of benzaldehyde or fairly strong Michael acceptors. Carbon dioxide (**1h**), thus, is not a weak electrophile, and it is the low thermodynamic driving force which accounts for its failure to react with a large variety of nucleophiles.

Rule of Thumb. Let us now use the reactivity parameters of eq 1 to summarize the synthetic potential of heteroallenes **1**. As s_N parameters are typically in the range of $0.7 < s_N < 1.0$, second-order rate constants from 10^{-4} to 10^{-3} M^{-1} s^{-1} at 20 °C can be expected for reactions of electrophiles with nucleophiles if $(E + N) = -4$. These rate constants correspond to a half reaction times of 1 h to half a day for 0.2 M solutions. Reactions with the highly nucleophilic alkyllithium and alkylmagnesium compounds with heteroallenes are well-known and will not explicitly be considered in the following discussion.

*Tosyl Isocyanate (**1b**, E = −7.69).* According to the Rule of Thumb, tosyl isocyanate (**1b**), the most reactive electrophile of this series, should undergo noncatalyzed reactions at room temperature with nucleophiles of $E > 4$. Thus, **1b** should react with all types of carbanions, as exemplified by the reaction of **1b** with the anion of diethyl 2-phenylmalonate (**2q**, N = 15.93) in THF (Table 6, entry 1).[22a] Products of the reactions of **1b** with enamines, which were used for the kinetic studies in this work (Tables 2 and 3) as illustrated for the reaction with 1-(N-

https://dx.doi.org/10.1021/jacs.0c01960
J. Am. Chem. Soc. XXXX, XXX, XXX−XXX

Table 5. Quantum Chemically Calculated Gibbs Reaction Energies Δ_rG^0 (kJ mol^{-1})[a] for the Reactions of Heteroallenes 1 with Carbanions 2a, 2n, and 2j (298 K, DMSO)

	2a		2n		2j	
	$\Delta_rG^0_{calcd}$ (IA)[b]	$\Delta_rG^0_{calcd}$ (TA)[c]	$\Delta_rG^0_{calcd}$ (IA)[b]	$\Delta_rG^0_{calcd}$ (TA)[c]	$\Delta_rG^0_{calcd}$ (IA)[b]	$\Delta_rG^0_{calcd}$ (TA)[c]
1a	−7	−36	34	−53	−21	−74
1b	−78	−63	−27	−69	−105	−98
1c	−26	−27	25	−40	−44	−68
1d	−48	−43	6	−54	−71	−93
1e	−9	−36	40	−45	−21	−72
1f	52	−24	93	−25	39	−41
1g	−24	3	21	−16	−56	−59
1h	−2	37	35	14	−19	−13

[a]Calculated at the IEFPCM(DMSO)/B3LYP-D3/6-311+G(d,p) level of theory. [b]$\Delta_rG^0_{calcd}$(**IA**) is the Gibbs reaction energy for formation of the initial adducts **IA**. [c]$\Delta_rG^0_{calcd}$(**TA**) is the Gibbs reaction energy for formation of the tautomeric adducts **TA**.

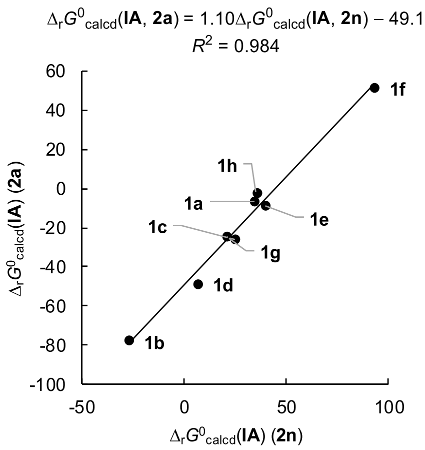

Figure 14. Correlation between Gibbs reaction energies $\Delta_rG^0_{calcd}$(**IA**) (kJ mol^{-1}) for the reactions of heteroallenes **1** with carbanions **2a** and **2n** calculated at the IEFPCM(DMSO)/B3LYP-D3/6-311+G(d,p) level of theory.

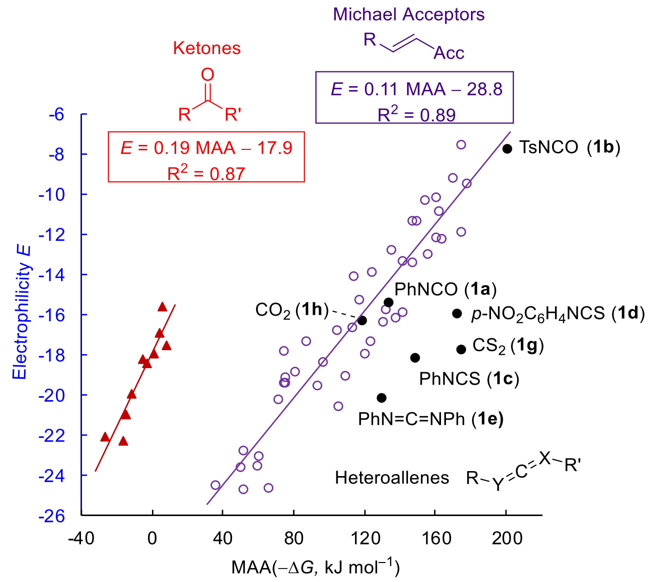

Figure 16. Correlation between electrophilicities E and MAA values (eq 2) calculated at SMD(DMSO)/B3LYP/6-311++G(3df,2pd)//B3LYP/6-31G(d,p) level of theory for ketones, Michael acceptors, and heteroallenes.

morpholino)cyclohexene (**3e**, N = 11.40) (Table 6, entry 2), have been reported previously.[12c,22b] We have found that **1b** undergoes electrophilic aromatic or vinylic substitutions with pyrroles (Table 6, entries 3 and 7) and the donor substituted fulvene **3h** (Table 6, entry 5), in line with Watt's report on uncatalyzed reactions of **1b** with N-alkylindoles ($N \approx 5.75$, Table 6, entry 8).[22c] No reaction was observed, however, when **1b** was combined with less nucleophilic arenes, such as 2-methylfuran (**3l**, N = 3.61) or 1,3-dimethoxybenzene (**3m**, N = 2.48) at 20 °C (Table 6, entries 9 and 10).

Apart from enamines also siloxy- and alkoxy-substituted ethylenes undergo noncatalyzed reactions with **1b**, as reported for the reactions with **3i** (N = 6.57, Table 6, entry 6), 1-(trimethylsiloxy)cyclohexene (N = 5.21),[22d] and 1,1-diethoxyethene (**3g**, N = 9.81, Table 6, entry 4).[22e] No reaction at ambient temperature was observed with the less nucleophilic α-methylstyrene (**3n**, N = 2.35, Table 6, entry 11), and the same is expected for other alkyl-substituted ethylenes.

Reactions of p-tosyl isocyanate (**1b**) with enol ethers have extensively been studied by Effenberger et al.[24] From stereochemical and kinetic investigations of the reactions of **1b** with

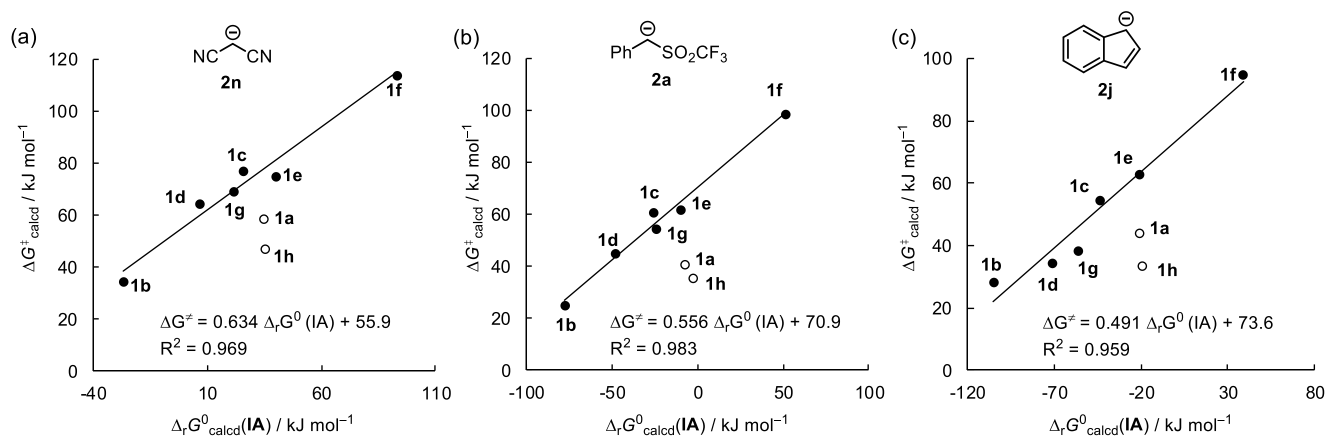

Figure 15. Correlations of Gibbs activation energies $\Delta G^{\ddagger}$ with Gibbs reaction energies Δ_rG^0(**IA**) for the reactions of heteroallenes **1** with **2n** (a), **2a** (b), and **2j** (c) calculated at the IEFPCM(DMSO)/B3LYP-D3/6-311+G(d,p) level of theory. Data for **1a** and **1h** were excluded when calculating the linear correlations.

https://dx.doi.org/10.1021/jacs.0c01960
J. Am. Chem. Soc. XXXX, XXX, XXX−XXX

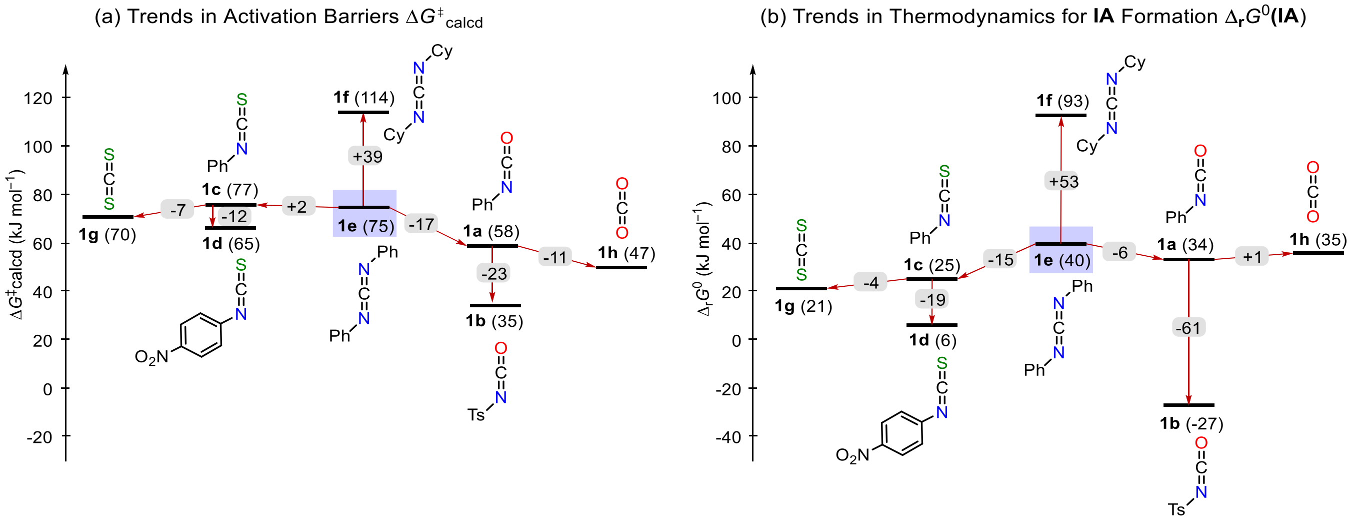

Figure 17. Structural effects on the Gibbs activation energies $\Delta G^{\ddagger}_{\text{calcd}}$ (a) and reaction energies $\Delta_r G^0_{\text{calcd}}$(**IA**) (b) for the reactions of heteroallenes **1** with the malononitrile anion (**2n**). The positive Gibbs reaction energies $\Delta_r G^0_{\text{calcd}}$(**IA**) imply that the thermodynamic driving force for many of these observable reactions comes from tautomerization of the initial adducts **IA** into **TA**.

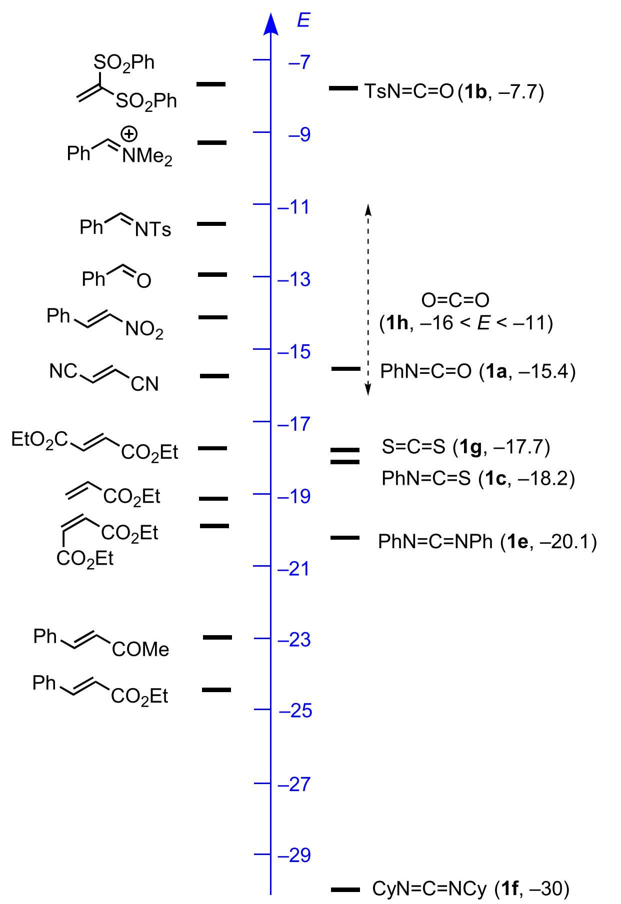

Figure 18. Comparison of electrophilicities of heteroallenes **1**, Michael acceptors, and carbonyl derivatives (E parameters from Table 3 and ref 10).

cis-/trans-isomeric enol ethers they concluded that the resulting azetidin-2-ones were formed via concerted [2+2] cycloadditions with partially charged transition states.[24d]

We have now investigated the reactions of **1b** with the enol ethers **3o** and **3p**, for which nucleophilicity parameters have previously been reported.[8a] As shown in Scheme 3, azetidin-2-ones with the donor substituents in 4-position were formed, as reported for **3o** and related enol ethers by Effenberger.[24a,b] Kinetic investigations by ^{1}H NMR spectroscopy showed that the reactions proceeded 5 times faster in CD_3CN than in CD_2Cl_2, indicating a moderate increase of polarity from reactants to the transition state (Table 7).

With the assumption that these reactions proceed stepwise with rate-determining formation of zwitterions, i.e., with formation of only one new σ-bond in the rate-determining step (Scheme 4), their rates should be predictable by eq 1. Table 7 shows that the rate constants $k_2^{\text{eq 1}}$ calculated by eq 1 are 4 to 8 times smaller than k_2^{exptl}, indicating a transition state which closely resembles the zwitterion depicted in Scheme 4.

Since the ratio $k_2^{\text{exptl}}/k_2^{\text{eq 1}}$ is within the uncertainty limits of eq 1, this small ratio does not allow to differentiate between a stepwise process and a concerted cycloaddition with a highly unsymmetrical transition state. Anyway, the small difference between k_2^{exptl} and $k_2^{\text{eq 1}}$ in Table 7 indicates that the electrophilicity parameter E for **1b** determined in this work can be used to predict absolute rate constants for [2+2] cycloadditions of **1b** with highly nucleophilic ethylene derivatives. Quantum chemical calculations support these conclusions and indicate initial formation of the CC-bond followed by a barrier-less subsequent ring closure (Supporting Information, Figure S31).

*Phenyl Isocyanate (**1a**, E = −15.38).* From the Rule of Thumb presented at the beginning of this section, one can derive that **1a** will react with nucleophiles of $N > 11$ at 20 °C. In line with this prediction numerous stabilized carbanions have been reported to react with **1a** at room temperature in different solvents, e.g., **2m**,[25a] **2n**,[25b] the anion of ethyl cyanoacetate (N = 19.62 in DMSO),[25c−f] the anion of diethyl 2-phenylmalonate (**2q**, N = 15.93),[25g] and the anion of ethyl 2-cyano-2-phenylacetate (N = 15.85).[25e]

There are several reports on the reactions of **1a** with enamines: 1-(N-morpholino)cyclohexene (**3e**, N = 11.40) reacted with **1a** at room temperature in benzene[26a,b] and under reflux in chloroform.[26c] 1-(N-Morpholino)cyclopentene (N = 13.41) smoothly underwent a reaction with **1a** at room temperature in acetone.[22b] The less nucleophilic α-(N-

Table 6. Reactions of *p*-Tosyl Isocyanate (1b) with Nucleophiles

Entry	Nucleophiles		N/s_N	$k_2^{eq\ 1}$ ($M^{-1}\ s^{-1}$)[a]	$t_{95\%}$[b]	Conditions	Products		Yields
1	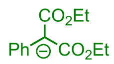	**2q**	15.93/0.99[c]	1.4×10^{8}	6.8×10^{-7} s	0.4 M, THF, rt, 4 h	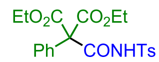	**4bq**	79% (ref 22a)
2	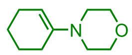	**3e**	11.40/0.83[d]	1.2×10^{3}	7.9×10^{-2} s	2 M, $CHCl_3$, rt, 90 min (or 0.25 M, CH_2Cl_2, −78 °C, 3 h, ref 12c)	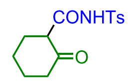	**4be**	62% (ref 22b)
3	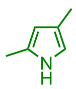	**3f**	10.67/0.91[e]	5.1×10^{2}	0.19 s	0.2 M, MeCN, 20 °C, 1 min	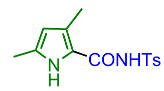	**4bf**	90%[k]
4	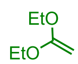	**3g**	9.81/0.81[f]	5.2×10^{1}	1.8 s	Et_2O, 20 °C, 10 min	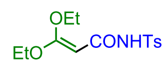	**4bg**	96% (ref 22e)
5	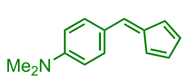	**3h**	6.72/0.87[g]	1.4×10^{-1}	11 min	0.2 M, MeCN, 20 °C, 11 min	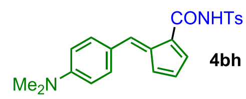	**4bh**	(ca 70%)[h,k]
6	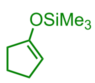	**3i**	6.57/0.93[d]	9.1×10^{-2}	17 min	no solvent, 15 min, rt	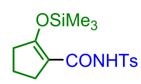	**4bi**	97% (ref 22d)
7		**3j**	5.85/1.03[d]	1.3×10^{-2}	2.0 h	0.2 M, CH_2Cl_2, 20 °C, 9.5 h	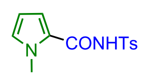	**4bj**	93%[k]
8	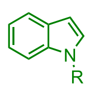	**3k**	5.75/1.23[i]	4.1×10^{-3}	6.4 h	0.4 M, Et_2O, rt, overnight or 0.4 M, toluene, 60–80 °C, overnight	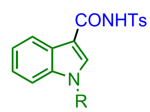	**4bk**	43–88% (ref 22c)
9	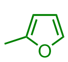	**3l**	3.61/1.11[d]	3.0×10^{-5}	37 d	0.2 M, CH_2Cl_2, 20 °C, 1 d	no reaction[k]		
10	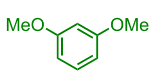	**3m**	2.48/1.09[d]	2.1×10^{-6}	524 d	0.2 M, CH_2Cl_2, 20 °C, 1 d	no reaction[k]		
11	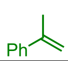	**3n**	2.35/1.00[j]	4.6×10^{-6}	239 d	0.2 M, CH_2Cl_2, 20 °C, 1 d	no reaction[k]		

[a]Calculated according to eq 1 with N and s_N parameters from this table and E(**1b**) from Table 3. [b]Calculated for 95% conversion with [**1b**] = [**3**] = 0.2 M. [c]In DMSO, from ref 23a. [d]In dichloromethane, from ref 8a. [e]In MeCN, from ref 23b. [f]In dichloromethane, from ref 23c. [g]In MeCN, from ref 23d. [h]The reaction furnished a 4:1 mixture of **4bh** and an unknown product (approximate yield refers to **4bh**). [i]For R = Me, in dichloromethane, from ref 23e. [j]In dichloromethane, from ref 8c. [k]This work.

Scheme 3. [2+2] Cycloadditions of 1b with Enol Ethers 3

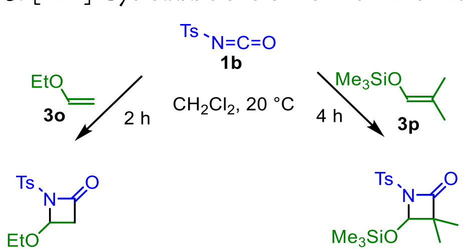

morpholino)styrene (N = 10.30) reacted with **1a** in cyclohexane at 80 °C within 30 min[22b] or in Et_2O at 5 °C within 24 h.[26d]

On the other hand, nucleophiles with N < 11 have been reported not to undergo uncatalyzed reactions with **1a** at room temperature. Effenberger, for example, mentioned that ordinary enol ethers do not react with phenyl isocyanate (**1a**) while 1,1-diethoxyethene (**3g**, N = 9.81) reacted with **1a** (neat) within 7 h

Table 7. Experimental and Calculated Second-Order Constants k_2 (in $M^{-1}\ s^{-1}$) of Reactions of *p*-Tosyl Isocyanate (1b) with Enol Ethers 3o and 3p in CD_2Cl_2 and CD_3CN (20 °C)

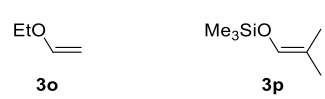

enol ether	N/s_N (in CH_2Cl_2)[a]	solvent	k_2^{exptl}	$k_2^{eq\ 1}$ [b]	$k_2^{exptl}/k_2^{eq\ 1}$
3o	3.92/0.90	CD_2Cl_2	1.6×10^{-3}	4.1×10^{-4}	3.9
		CD_3CN	8.0×10^{-3}		
3p	3.94/1.00	CD_2Cl_2	1.5×10^{-3}	1.8×10^{-4}	8.3
		CD_3CN	7.0×10^{-3}		

[a]From ref 8a [b]Calculated by using eq 1, N and s_N, and E(**1b**) = −7.69 (from Table 3).

https://dx.doi.org/10.1021/jacs.0c01960
J. Am. Chem. Soc. XXXX, XXX, XXX−XXX

Scheme 4. Hypothetical Stepwise [2+2] Cycloaddition of 1b with Enol Ethers

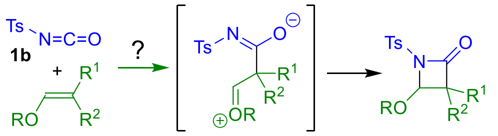

Scheme 5. Piperidine-Catalyzed Reaction of Meldrum's Acid with 1f (as Reported in Ref 32)

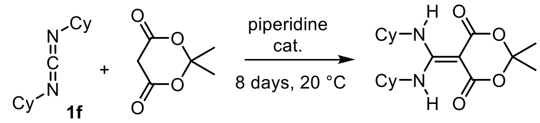

at 100 °C.[22e] Whereas the reactions of silyl enol ethers with *p*-tosyl isocyanate (**1b**) proceeded smoothly at room temperature[24] (Scheme 3), heating at 130−160 °C in the presence of a catalytic amount of tertiary amine was required to achieve the reactions of **1a** with **3i** (N = 6.57) and 1-(trimethylsiloxy)-cyclohexene (N = 5.21).[22d] Furthermore, the reaction of **1a** with *N*-methylindole (N = 5.75) was reported to require Me_2AlCl as catalyst,[27a] and Ni(0) catalysis was used to enable the reaction of **1a** with cyclopentene (N = −1.55).[27b]

Phenyl Isothiocyanate (1c, E = −18.15). Because of its lower electrophilicity, compared with its O-analog **1a**, phenyl isothiocyanate reacts only with stronger nucleophiles (N > 14). At room temperature, reactions of **1c** with the anion of phenylacetonitrile (N ≈ 29),[28a] the anions of methyl phenylacetate (N ≈ 27.5),[28b] of alkyl cyanoacetate (N ≈ 19.6),[28c−e] of 1-phenylbutane-1,3-dione (N = 16.03),[28f,g] of diethyl cyanomethylphosphonate (N = 18.57), and of triethyl phosphonoacetate (N = 19.23) in diethyl ether have previously been reported.[28h] Furthermore, mixtures of **1c** with anionic C-nucleophiles such as **2m−p** (generated from the corresponding CH acids and potassium carbonate in DMF) and iodomethane have been described to yield ketene-*N*,*S*-acetals at room temperature.[13]

Moderately reactive enamines were reported to react with **1c** at elevated temperature. Thus, 1-(*N*-morpholino)cyclopentene (N = 13.41) reacted with **1c** in chloroform under reflux,[26c] and the weakly nucleophilic α-(*N*-morpholino)styrene (N = 10.30) reacted with **1c** in EtOAc under reflux for 1 h.[22b] Harsh reaction conditions were needed for the reactions of ketene acetals (N ≈ 10) with **1c**.[29] Thus, the [2+2] cycloaddition of 1,1-dimethoxy-2-methylprop-1-ene across the C═N bond of **1c** was reported to take place when equimolar amounts of the two reactants were heated without a solvent for 3 days at 100 °C.[29]

As expected from their low nucleophilicities, toluene (N = −4.36), furan (N = 1.33), and pyrrole (N = 4.63) do not undergo uncatalyzed reactions with **1c**.[30] These arenes can be converted into the corresponding aromatic thioamides, however, by heating them with phenyl isothiocyanate (**1c**) in cyclohexane solution with stoichiometric amounts of $AlCl_3$.[30]

Diphenylcarbodiimide (1e, E = −20.14). In line with the predictions of the linear free-energy relationship (eq 1), reactions of **1e** with various carbanions have been reported previously,[31a,b] including reactions with **2m** (N = 20.22),[31c] **2n** (N = 19.36),[31d] the anion of ethyl cyanoacetate (N = 19.62),[31b,d] the anion of 1,3-diphenylpropane-1,3-dione (N = 17.46),[31d] and the anion of ethyl 3-oxo-3-phenylpropanoate (N = 17.52),[31d] while trimethylsulfoxonium ylide (N = 21.29)[31e] was the only neutral C-nucleophile which was reported to undergo uncatalyzed reactions with **1e**.

Dicyclohexylcarbodiimide (1f, E ≈ −30). As mentioned in Table 3, the electrophilicity of **1f** is so low that it did not even react with the highly nucleophilic carbanion **2e** (N = 27.54) when generated by deprotonation of ethyl phenylacetate with KO*t*Bu in DMSO. In view of this observation, the report by Stephen[32] that **1f** reacted with the much less nucleophilic anion of Meldrum's acid (N = 13.91) appears surprising (Scheme 5).

However, in line with the observations described in Table 3, no reaction was observed within 12 days at ambient temperature when we treated **1f** with 1.1 equiv of an equimolar mixture of Meldrum's acid and KO*t*Bu in d_6-DMSO. On the other hand, following the conditions of Stephen, i.e., when we treated an equimolar mixture of Meldrum's acid and **1f** with a few drops of piperidine in $CDCl_3$ (Scheme 5) we observed the quantitative formation of an adduct within 4 days at room temperature. Thus, the nucleophilic attack of the anion of Meldrum's acid at **1f** is possible when a proton source (piperidinium ion) is available. In contrast, the acidity of *tert*-butanol (formed from Meldrum's acid and KO*t*Bu) is obviously not sufficient to assist the nucleophilic attack at **1f**. In line with these findings, the formation of peptide bonds by **1f**-promoted coupling of carboxylic acids with amines proceeds via initial protonation of **1f** followed by nucleophilic attack of the carboxylate anion at the protonated carbodiimide.[21]

Carbon Disulfide (1g, E = −17.70). CS_2 is a stronger Lewis acid but a weaker electrophile than CO_2 (Figure 17) and can be attacked by nucleophiles with N > 14. It was reported to react with *N*-heterocyclic carbenes, e.g., 1,3-dimesitylimidazolylidene (N = 21.72) in THF at room temperature to form the zwitterionic dithiocarboxylates.[33] Several pyridinium ylides (N > 18)[10] were also reported to react with CS_2 in EtOH at room temperature.[34] The sodium salts of diethyl cyanomethylphosphonate (N = 18.57) and of triethyl phosphonoacetate (N = 19.23) were reported to react with **1g** in THF at room temperature.[35] Cyclic enamines (N > 14) were found to react with CS_2 at −30 °C yielding 1,4-dipoles that can be stored for 1 day at 0 °C in the absence of moisture.[36]

Carbon Dioxide (1h). The prediction of reactions of CO_2 on the basis of eq 1 is problematic for two reasons. First, the experimentally derived electrophilicity E(**1h**) = −16.3 is based on the rate of reaction of CO_2 with only one nucleophile (**2j**). Second, the questionable transferability of this number has been discussed above. However, since quantum chemical calculations indicate an even higher electrophilicity of CO_2 (E = −11), the value derived from the rate of its reaction with **2j** can be considered as the lower limit with the consequence that nucleophiles with N > 12 should generally be able to attack at CO_2. The failure to obtain products with a variety of highly nucleophilic carbanions (Supporting Information, Chart S1), may therefore be caused by the unfavorable thermodynamics of these reactions. The thermodynamic driving force is sufficient, however, for reactions with the highly reactive alkyllithium and alkylmagnesium compounds.[6b] In line with its nucleophilicity parameter, the *N*-heterocyclic carbene 1,3-dimesitylimidazolylidene (N = 21.72) reacted with 1 atm CO_2 in THF at room temperature to give a zwitterionic adduct.[37] *N*-Methylindole (N = 5.75) and *N*-methyl pyrrole (**3j**, N = 5.85) are not sufficiently nucleophilic to attack CO_2, but their Lewis acid-catalyzed reactions have been reported.[27a,38] Though the intensively investigated reactions of carbon dioxide with amines may proceed via different catalyzed and uncatalyzed mechanisms to give ammonium carbamates,[39] most secondary amines

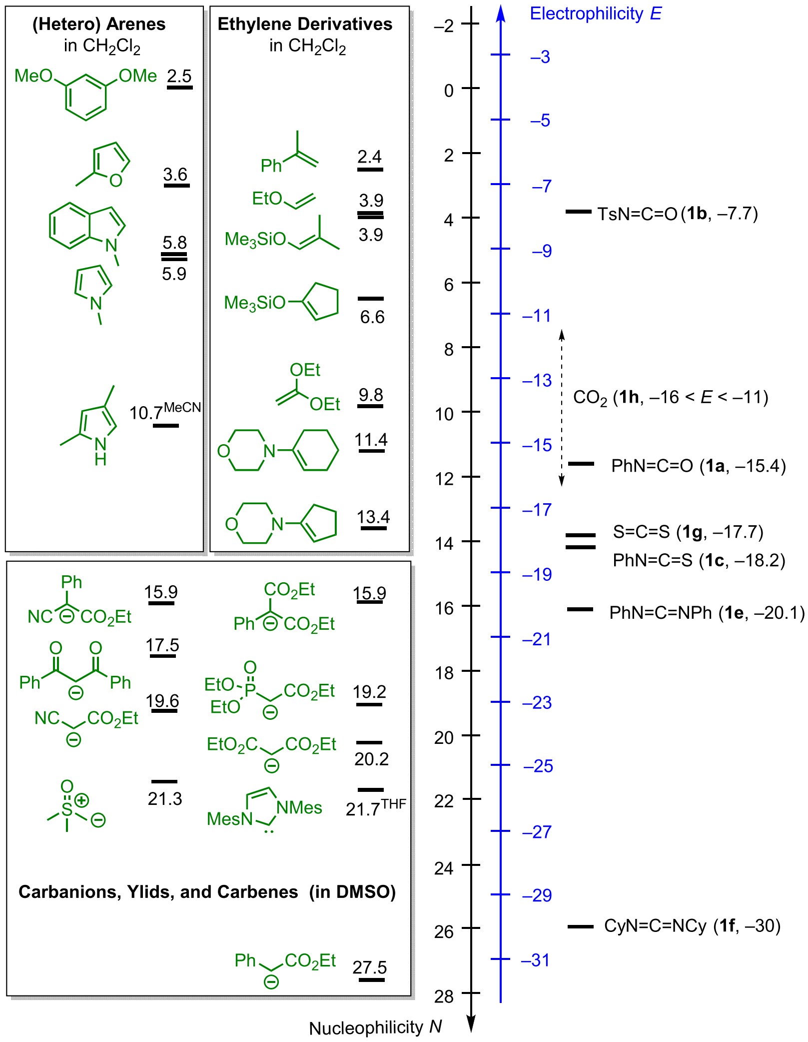

Figure 19. Graphical summary of the synthetic potential of heteroallenes **1**.

are able to undergo uncatalyzed reactions with CO_2 due to their N-values in the range $14 < N < 18$.[10]

■ CONCLUSION

The photometrically determined second-order rate constants for the reactions of heteroallenes **1** with the carbanions **2** and enamines **3** in DMSO or acetonitrile follow the linear free-energy relationship eq 1, which allowed us to determine the electrophilicity parameters E of heteroallenes. As depicted in Figure 18, tosyl isocyanate (**1b**, $E = -7.69$), the most reactive heteroallene of this series, is 8 orders of magnitude more reactive than phenyl isocyanate (**1a**, $E = -15.38$), which has an electrophilicity comparable to *trans*-1,2-dicyanoethylene. Phenyl isothiocyanate (**1c**, $E = -18.15$) and carbon disulfide (**1f**, $E = -17.70$) are more than 2 orders of magnitude less reactive, and there is another hundred-fold decrease of electrophilicity to diphenylcarbodiimide (**1e**, $E = -20.14$). The electrophilicity of dicyclohexylcarbodiimide (**1f**) is so low that we do not have suitable reference nucleophiles for measuring its reactivity, and its approximate electrophilicity $E \approx -30$ was derived by quantum chemical calculations. The electrophilicity of CO_2 could not unambiguously be quantified, but the accessible experimental data and quantum chemical calculations agree that CO_2 is not a weak electrophile. Its reactivity is comparable to that of benzaldehyde. The failure of CO_2 to give products with a large variety of sufficiently strong nucleophiles is due to a lack of thermodynamic driving force.

The reactivities of CO_2 and CS_2 as well as those of phenyl isocyanate and phenyl isothiocyanate toward nucleophiles were investigated by quantum-chemical methods applying the distortion interaction analysis. The higher demand of distortion energy for the CS_2 fragment explains the lower reactivity of CS_2 compared with CO_2 in analogous reactions though nucleophiles form the more stable adducts with CS_2. Nucleophiles approach the heteroallenes PhNCO and PhNCS by *anti* or *syn* pathways, with the lower calculated Gibbs energies of activation for the *syn* attack. In analogy to the relative reactivities of CO_2/CS_2, it is the lower distortion energy of PhNCO which makes it the stronger electrophile though PhNCS reacts more exergonically with nucleophiles.

The satisfactory agreement between quantum chemically calculated Gibbs activation energies and experimental values confirms the internal consistency of our data and allowed us to investigate rate-equilibrium relationships. Earlier studies showed fair correlations between the electrophilicities of acceptor-substituted ethylenes and ketones with calculated methyl anion affinities (MAAs).[20] The analogous E vs MAA correlation for the heteroallenes is very poor, due to the large structural diversity of the investigated heteroallenes. The fact that heteroallenes are generally less electrophilic than ketones

https://dx.doi.org/10.1021/jacs.0c01960
J. Am. Chem. Soc. XXXX, XXX, XXX−XXX

and Michael acceptors of comparable MAA implies that cumulated double bonds react over higher intrinsic barriers than ordinary double bonds.

The reactivity parameters in eq 1 have been derived from reactions of electrophiles with nucleophiles, in which one, and only one, new bond is formed in the rate-determining step. For that reason, eq 1 is generally not applicable to multi-bond reactions. However, when the one-bond electrophilicity E of *p*-tosyl isocyanate (**1b**) and the one-bond nucleophilicity parameters N and s_N of enol ethers are applied in eq 1, second-order rate constants are calculated which closely resemble those which have been measured for the [2+2] cycloadditions of these reactants. Hence, this work adds another example to the observation that the one-bond reactivity parameters E, N and s_N can also be used for predicting absolute rate constants for stepwise or highly unsymmetrical concerted cycloadditions.[40]

As s_N parameters of C-nucleophiles are typically in the range of $0.7 < s_N < 1.0$, second-order rate constants from 10^{-4} to 10^{-3} M^{-1} s^{-1} at 20 °C can be expected for reactions of electrophiles with C-nucleophiles if $(E + N) = -4$. Since these rate constants correspond to a half reaction times of 1 h to half a day for 0.2 M solutions, one can summarize the synthetic potential of heteroallenes semiquantitatively as shown in Figure 19: Heteroallenes **1** will undergo uncatalyzed reactions at 20 °C with those nucleophiles which are positioned below themselves in Figure 19, provided there is sufficient thermodynamic driving force.

■ ASSOCIATED CONTENT

Supporting Information

The Supporting Information is available free of charge at https://pubs.acs.org/doi/10.1021/jacs.0c01960.

Synthetic procedures, details of kinetic measurements, procedure for the preparation of CO_2 solutions in DMSO, details of quantum-chemical calculations, and NMR spectra of all characterized compounds (PDF)

Coordinates of optimized structures (ZIP)

■ AUTHOR INFORMATION

Corresponding Authors

Armin R. Ofial − *Department Chemie, Ludwig-Maximilians-Universität München, 81377 München, Germany;* orcid.org/0000-0002-9600-2793; Email: ofial@lmu.de

Herbert Mayr − *Department Chemie, Ludwig-Maximilians-Universität München, 81377 München, Germany;* orcid.org/0000-0003-0768-5199; Email: herbert.mayr@cup.uni-muenchen.de

Authors

Zhen Li − *Department Chemie, Ludwig-Maximilians-Universität München, 81377 München, Germany*

Robert J. Mayer − *Department Chemie, Ludwig-Maximilians-Universität München, 81377 München, Germany*

Complete contact information is available at: https://pubs.acs.org/10.1021/jacs.0c01960

Notes

The authors declare no competing financial interest.

■ ACKNOWLEDGMENTS

Dedicated to Professor Reinhard Brückner on the occasion of his 65th birthday. We thank the China Scholarship Council (fellowship to Z.L.) and the Fonds der Chemischen Industrie (Kekulé fellowship to R.J.M.) for financial support.

■ REFERENCES

(1) (a) Ulrich, H. *Cumulenes In Click Reactions*, 1st ed.; Wiley: New York, 2010. (b) Brandsma, L. Unsaturated Carbanions, Heteroallenes and Thiocarbonyl Compounds − New Routes to Heterocycles. *Eur. J. Org. Chem.* **2001**, 4569−4581. (c) Louie, J. Transition Metal Catalyzed Reactions of Carbon Dioxide and Other Heterocumulenes. *Curr. Org. Chem.* **2005**, *9*, 605−623. (d) Schenk, S.; Notni, J.; Köhn, U.; Wermann, K.; Anders, E. Carbon dioxide and related heterocumulenes at zinc and lithium cations: bioinspired reactions and principles. *Dalton Trans* **2006**, 4191−4206. (e) Braverman, S.; Cherkinsky, M.; Birsa, M. L. Carbon dioxide, carbonyl sulfide, carbon disulfide, isocyanates, isothiocyanates, carbodiimides, and their selenium, tellurium, and phosphorus analogues. In *Science of Synthesis*; Knight, J. G., Ed.; Thieme: Stuttgart, Germany, 2005; Vol. *18*, pp 65−320.

(2) (a) Ozaki, S. Recent Advances in Isocyanate Chemistry. *Chem. Rev.* **1972**, *72*, 457−496. (b) Arnold, R. G.; Nelson, J. A.; Verbanc, J. J. Recent Advances in Isocyanate Chemistry. *Chem. Rev.* **1957**, *57*, 47−76. (c) Rasmussen, J. K.; Hassner, A. Recent Developments in the Synthetic Uses of Chlorosulfonyl Isocyanate. *Chem. Rev.* **1976**, *76*, 389−408. (d) Giles, D. E. Kinetics and mechanisms of reactions of cyanates and related compounds. In *The Chemistry of Cyanates and Their Thio Derivatives, Part 1, Vol. 1*; Patai, S., Ed.; Wiley: Chichester, UK, 1977; Chapter 12, pp 381−444. (e) Richter, R.; Ulrich, H. Synthesis and preparative applications of isocyanates. In *The Chemistry of Cyanates and Their Thio Derivatives, Part 2, Vol. 2*; Patai, S., Ed.; Wiley: Chichester, UK, 1977; Chapter 17, pp 619−818. (f) Ulrich, H. *Chemistry and Technology of Isocyanates*, 1st ed.; Wiley: Chichester, UK, 1996. (g) Huang, D.; Yan, G. Recent advances in reactions of aryl sulfonyl isocyanates. *Org. Biomol. Chem.* **2017**, *15*, 1753−1761. (h) King, C. Some Reactions of p-Toluenesulfonyl Isocyanate. *J. Org. Chem.* **1960**, *25*, 352−356.

(3) (a) Mukerjee, A. K.; Ashare, R. Isothiocyanates in the Chemistry of Heterocycles. *Chem. Rev.* **1991**, *91*, 1−24. (b) Assony, S. J. The Chemistry of Isothiocyanates. In *Organic Sulfur Compounds*; Kharasch, N., Ed.; Pergamon Press: New York, 1961; Chapter 28, pp 326−338. (c) Trofimov, B. A. Reactions of Unsaturated Carbanions with Isothiocyanates: A New Avenue to Fundamental Heterocycles. *J. Heterocycl. Chem.* **1999**, *36*, 1469−1490. (d) Pace, V.; Monticelli, S.; de la Vega-Hernandez, K.; Castoldi, L. Isocyanates and isothiocyanates as versatile platforms for accessing (thio)amide-type compounds. *Org. Biomol. Chem.* **2016**, *14*, 7848−7854. (e) Frankowski, S.; Więckowska, A.; Albrecht, Ł. Iso(thio)cyanate-strategy for the organocatalytic synthesis of selected heterocyclic structures. *Targets in Heterocyclic Systems*; Società Chimica Italiana, 2018; Vol. *22*, pp 298−317 (f) Eschliman, K.; Bossmann, S. H. Synthesis of Isothiocyanates: An Update. *Synthesis* **2019**, *51*, 1746−1752.

(4) (a) Williams, A.; Ibrahim, I. T. Carbodiimide Chemistry: Recent Advances. *Chem. Rev.* **1981**, *81*, 589−636. (b) Ulrich, H. *Chemistry and Technology Carbodiimides*, 1st ed.; Wiley: West Sussex, UK, 2007.

(5) (a) Yokoyama, M.; Imamoto, T. Organic Reactions of Carbon Disulfide. *Synthesis* **1984**, 797−824. (b) Rudorf, W. D. Reactions of Carbon Disulfide with C-nucleophiles. *Sulfur Rep.* **1991**, *11*, 51−141. (c) Rudorf, W. D. Reactions of carbon disulfide with N-nucleophiles. *J. Sulfur Chem.* **2007**, *28*, 295−339. (d) Iglesias-Sigüenza, F. J. Carbon Disulfide (CS_2). *Synlett* **2009**, 157−158.

(6) (a) Sakakura, T.; Choi, J.-C.; Yasuda, H. Transformation of Carbon Dioxide. *Chem. Rev.* **2007**, *107*, 2365−2387. (b) Liu, Q.; Wu, L.; Jackstell, R.; Beller, M. Using carbon dioxide as a building block in organic synthesis. *Nat. Commun.* **2015**, *6*, 5933.

(7) (a) Aresta, M. *Carbon Dioxide as Chemical Feedstock*; Wiley-VCH: Weinheim, 2010. (b) Centi, G.; Perathoner, S. *Green Carbon Dioxide: Advances in CO_2 Utilization*; Wiley-VCH: Weinheim, 2014. (c) Artz, J.;

Muller, T. E.; Thenert, K.; Kleinekorte, J.; Meys, R.; Sternberg, A.; Bardow, A.; Leitner, W. Sustainable Conversion of Carbon Dioxide: An Integrated Review of Catalysis and Life Cycle Assessment. *Chem. Rev.* **2018**, *118*, 434−504. (d) Arnold, P. L.; Kerr, R. W. F.; Weetman, C.; Docherty, S. R.; Rieb, J.; Cruickshank, F. L.; Wang, K.; Jandl, C.; McMullon, M. W.; Pöthig, A.; Kühn, F. E.; Smith, A. D. Selective and catalytic carbon dioxide and heteroallene activation method by cerium N-heterocyclic carbene complexes. *Chem. Sci.* **2018**, *9*, 8035−8045. (e) Sen, R.; Goeppert, A.; Kar, S.; Prakash, G. K. S. Hydroxide Based Integrated CO_2 Capture from Air and Conversion to Methanol. *J. Am. Chem. Soc.* **2020**, *142*, 4544−4549.

(8) (a) Mayr, H.; Bug, T.; Gotta, M. F.; Hering, N.; Irrgang, B.; Janker, B.; Kempf, B.; Loos, R.; Ofial, A. R.; Remennikov, G.; Schimmel, H. Reference Scales for the Characterization of Cationic Electrophiles and Neutral Nucleophiles. *J. Am. Chem. Soc.* **2001**, *123*, 9500−9512. (b) Lucius, R.; Loos, R.; Mayr, H. Kinetics of carbocation-carbanion combinations: Key to a General Concept of Polar Organic Reactivity. *Angew. Chem., Int. Ed.* **2002**, *41*, 91−95. (c) Mayr, H.; Kempf, B.; Ofial, A. R. π-Nucleophilicity in Carbon-Carbon Bond-Forming Reactions. *Acc. Chem. Res.* **2003**, *36*, 66−77. (d) Mayr, H.; Ofial, A. R. A Quantitative Approach to Polar Organic Reactivity. *SAR QSAR Environm. Res.* **2015**, *26*, 619−646.

(9) (a) Berger, S. T. A.; Ofial, A. R.; Mayr, H. Inverse Solvent Effects in Carbocation Carbanion Combination Reactions: The Unique Behavior of Trifluoromethylsulfonyl Stabilized Carbanions. *J. Am. Chem. Soc.* **2007**, *129*, 9753−9761. (b) Timofeeva, D. S.; Ofial, A. R.; Mayr, H. Kinetics of Electrophilic Fluorinations of Enamines and Carbanions: Comparison of the Fluorinating Power of N-F Reagents. *J. Am. Chem. Soc.* **2018**, *140*, 11474−11486. (c) Corral-Bautista, F.; Mayr, H. Quantification of the Nucleophilic Reactivities of Ethyl Arylacetate Anions. *Eur. J. Org. Chem.* **2013**, 4255−4261. (d) Kaumanns, O.; Appel, R.; Lemek, T.; Seeliger, F.; Mayr, H. Nucleophilicities of the Anions of Arylacetonitriles and Arylpropionitriles in Dimethyl Sulfoxide. *J. Org. Chem.* **2009**, *74*, 75−81. (e) Corral-Bautista, F.; Klier, L.; Knochel, P.; Mayr, H. From Carbanions to Organometallic Compounds: Quantification of Metal Ion Effects on Nucleophilic Reactivities. *Angew. Chem., Int. Ed.* **2015**, *54*, 12497−12500. (f) Seeliger, F.; Mayr, H. Nucleophilic reactivities of benzenesulfonyl-substituted carbanions. *Org. Biomol. Chem.* **2008**, *6*, 3052−3058. (g) Lemek, T.; Mayr, H. Electrophilicity Parameters for Benzylidenemalononitriles. *J. Org. Chem.* **2003**, *68*, 6880−6886. (h) Timofeeva, D. S.; Mayer, R.; Mayer, P.; Ofial, A.; Mayr, H. Which Factors Control the Nucleophilic Reactivities of Enamines? *Chem. - Eur. J.* **2018**, *24*, 5901−5910.

(10) For a comprehensive database of nucleophilicity parameters N and s_N as well as electrophilicity parameters E, see http://www.cup.lmu.de/oc/mayr/DBintro.html.

(11) (a) Opitz, G.; Koch, J. β-Amino-β-lactams. *Angew. Chem., Int. Ed. Engl.* **1963**, *2*, 152. (b) Schaumann, E.; Sieveking, S.; Walter, W. Darstellung stabiler 1,4-Dipole aus β,β-Dialkyl-enaminen und Sulfonylisocyanaten. *Tetrahedron Lett.* **1974**, *15*, 209−212.

(12) (a) Shvydenko, T.; Nazarenko, K.; Shvydenko, K.; Boron, S.; Gutov, O.; Tolmachev, A.; Kostyuk, A. Reduction of imidazolium salts − An approach to diazocines and diazocanes. *Tetrahedron* **2017**, *73*, 6942−6953. (b) Lyutenko, N. V.; Gerus, I. I.; Kacharov, A. D.; Kukhar, V. P. Regioselective reactions of β-aminovinyl trifluoromethyl ketones with tosyl isocyanate. *Tetrahedron* **2003**, *59*, 1731−1738. (c) Sugiura, M.; Kashiwagi, T.; Ito, M.; Kotani, S.; Nakajima, M. Stereoselective Synthesis of Nitrogen-Containing Compounds from Enamines. *J. Org. Chem.* **2017**, *82*, 10968−10979. (d) Kostyuk, A. N; Volochnyuk, D. M; Lupihal, L. N; Pinchuk, A. M; Tolmachev, A. A Electrophilic substitution as a convenient approach to functionalized *N*-benzyl-1,4-dihydropyridines. *Tetrahedron Lett.* **2002**, *43*, 5423−5425. (e) Vilsmaier, E.; Adam, R.; Altmeier, P.; Fath, J.; Scherer, H. J.; Maas, G.; Wagner, O. Functionalized chloroenamines in aminocyclopropane synthesis IV A synthesis for bicyclic lactams from carbamoylated chloroenamines - the result of a tandem ring contraction − cyclization process. *Tetrahedron* **1989**, *45*, 6683−6696.

(13) Sommen, G.; Comel, A.; Kirsch, G. Preparation of thieno[2,3-*b*]pyrroles from ketene-*N*,*S*-acetals. *Tetrahedron* **2003**, *59*, 1557−1564.

(14) (a) Chiba, K.; Tagaya, H.; Miura, S.; Karasu, M. The Carboxylation of Active Methylene Compounds with Carbon Dioxide in the Presence of 18-Crown-6 and Potassium Carbonate. *Chem. Lett.* **1992**, *21*, 923−926. (b) Fluorene (pK_a = 22.6 in DMSO, ref 14c) is a weaker Brønsted acid than indene (pK_a = 20.1 in DMSO, ref 14d), which suggests that the fluorenide anion is slightly more nucleophilic than the indenide anion. (c) Matthews, W. S.; Bares, J. E.; Bartmess, J. E.; Bordwell, F. G.; Cornforth, F. J.; Drucker, G. E.; Margolin, Z.; McCallum, R. J.; McCollum, G. J.; Vanier, N. R. Equilibrium Acidities of Carbon Acids. VI. Establishment of an Absolute Scale of Acidities in Dimethyl Sulfoxide Solution. *J. Am. Chem. Soc.* **1975**, *97*, 7006−7014. (d) Bordwell, F. G.; Drucker, G. E. Acidities of Indene and Phenyl-, Diphenyl-, and Triphenylindenes. *J. Org. Chem.* **1980**, *45*, 3325−3328.

(15) (a) Hua, L. Thermodynamic model of solubility for CO_2 in dimethyl sulfoxide. *Phys. Chem. Liq.* **2009**, *47*, 296−301. (b) The CO_2 concentration of a dilute DMSO solution determined by titration with NaOH standard solution using phenolphthalein as indicator was 6% higher (averaged from three titrations) than that calculated by our standard method by applying Henry's law for the solubility of CO_2 in DMSO under atmospheric pressure of CO_2 (Supporting Information).

(16) (a) Becke, A. D. Density-functional thermochemistry. III. The role of exact exchange. *J. Chem. Phys.* **1993**, *98*, 5648−5652. (b) Cances, E.; Mennucci, B.; Tomasi, J. A new integral equation formalism for the polarizable continuum model: Theoretical background and applications to isotropic and anisotropic dielectrics. *J. Chem. Phys.* **1997**, *107*, 3032−3041. (c) Grimme, S.; Antony, J.; Ehrlich, S.; Krieg, H. A consistent and accurate *ab initio* parametrization of density functional dispersion correction (DFT-D) for the 94 elements H-Pu. *J. Chem. Phys.* **2010**, *132*, 154104. (d) Visualized with the CYLview software package: Legault, C. Y. *CYLview, 1.0b*; Université de Sherbrooke, 2009. http://www.cylview.org (e) Visualized with the IboView software package: Knizia, G. Intrinsic Atomic Orbitals: An Unbiased Bridge Between Quantum Theory and Chemical Concepts. *J. Chem. Theory Comput.* **2013**, *9*, 4834−4843.

(17) Bickelhaupt, F. M.; Houk, K. N. Analyzing Reaction Rates with the Distortion/Interaction-Activation Strain Model. *Angew. Chem., Int. Ed.* **2017**, *56*, 10070−10086.

(18) Bernasconi, C. F.; Zitomer, J. L.; Fox, J. P.; Howard, K. A. Nucleophilic Addition to Olefins. 9.[1] Kinetics of the Reaction of Benzylidenemalononitrile with Malononitrile Anion. *J. Org. Chem.* **1984**, *49*, 482−486.

(19) (a) Jencks, W. P. A primer for the Bema Hapothle. An empirical approach to the characterization of changing transition-state structures. *Chem. Rev.* **1985**, *85*, 511−527. (b) Leffler, J. E. Parameters for the Description of Transition States. *Science* **1953**, *117*, 340−341. (c) Pross, A. Rate-equilibrium relationships. In *Theoretical and physical principles of organic reactivity*; Pross, A., Ed.; Wiley: Chichester, UK, 1995; pp 175−182.

(20) (a) Allgäuer, D. S.; Jangra, H.; Asahara, H.; Li, Z.; Chen, Q.; Zipse, H.; Ofial, A. R.; Mayr, H. Quantification and Theoretical Analysis of the Electrophilicities of Michael Acceptors. *J. Am. Chem. Soc.* **2017**, *139*, 13318−13329. (b) Li, Z.; Jangra, H.; Chen, Q.; Mayer, P.; Ofial, A. R.; Zipse, H.; Mayr, H. Kinetics and Mechanism of Oxirane Formation by Darzens Condensation of Ketones: Quantification of the Electrophilicities of Ketones. *J. Am. Chem. Soc.* **2018**, *140*, 5500−5515. (c) Mayer, R. J.; Ofial, A. R. Nucleophilicity of Glutathione: A Link to Michael Acceptor Reactivities. *Angew. Chem., Int. Ed.* **2019**, *58*, 17704−17708. (d) For a recent survey of MAA-based reactivity predictions for other functional groups, see: Mood, A. D.; Tavakoli, M.; Gutman, E. S.; Kadish, D.; Baldi, P.; Van Vranken, D. L. Methyl Anion Affinities of the Canonical Organic Functional Groups. *J. Org. Chem.* **2020**, *85*, 4096−4102.

(21) Carey, F. A.; Sundberg, R. J. *Advanced Organic Chemistry Part B: Reactions and Synthesis*, 5th ed.; Springer: New York, 2007; p 247.

(22) (a) Gololobov, Y. G.; Slepchenkov, N. V.; Petrovskii, P. V.; Nelyubina, Y. V. On the nature of intermediates in the reactions of carbanions of diethyl arylmalonates with isocyanates. *Russ. Chem. Bull.* **2009**, *58*, 1088−1090. (b) Hünig, S.; Hübner, K.; Benzing, E. Addition von Isocyanaten und Isothiocyanaten an Enamine. *Chem. Ber.* **1962**, *95*,

926–936. (c) Watt, M. S.; Booker-Milburn, K. I. Palladium(II) Catalyzed C-H Functionalization Cascades for the Diastereoselective Synthesis of Polyheterocycles. *Org. Lett.* **2016**, *18*, 5716–5719. (d) Inaba, S.-I.; Ojima, I.; Yoshida, K.; Nagai, M. Reactions of Silyl Enol Ethers and Ketene Silyl Ketals with Isocyanates. *J. Organomet. Chem.* **1979**, *164*, 123–134. (e) Effenberger, F.; Gleiter, R.; Kiefer, G. Vergleichende Reaktionen von Isocyanaten mit Ketenacetalen, Keten-*O.N*-acetalen und Keten-*N.N*-acetalen. *Chem. Ber.* **1966**, *99*, 3892–3902.

(23) (a) Puente, A.; Ofial, A. R.; Mayr, H. Nucleophilic Reactivities of Bis-Acceptor-Substituted Benzyl Anions. *Eur. J. Org. Chem.* **2017**, 1196–1202. (b) Nigst, T. A.; Westermaier, M.; Ofial, A. R.; Mayr, H. Nucleophilic Reactivities of Pyrroles. *Eur. J. Org. Chem.* **2008**, 2369–2374. (c) Tokuyasu, T.; Mayr, H. Nucleophilic Reactivities of Ketene Acetals. *Eur. J. Org. Chem.* **2004**, 2791–2796. (d) Kedziorek, M.; Mayer, P.; Mayr, H. Nucleophilic Reactivities of Azulene and Fulvenes. *Eur. J. Org. Chem.* **2009**, 1202–1206. (e) Lakhdar, S.; Westermaier, M.; Terrier, F.; Goumont, R.; Boubaker, T.; Ofial, A. R.; Mayr, H. Nucleophilic Reactivities of Indoles. *J. Org. Chem.* **2006**, *71*, 9088–9095.

(24) (a) Effenberger, F.; Gleiter, R. The Reaction of Sulfonyl Isocyanates with Vinyl Ethers. *Angew. Chem., Int. Ed. Engl.* **1963**, *2*, 324. (b) Effenberger, F.; Gleiter, R. Reaktion von Sulfonylisocyanaten mit Enoläthern. *Chem. Ber.* **1964**, *97*, 1576–1583. (c) Effenberger, F.; Fischer, P.; Prossel, G.; Kiefer, G. Stereospezifische Cycloaddition von Sulfonylisocyanaten an Enoläther – Konfiguration, Isomerisierung und Umlagerung der Cycloaddukte. *Chem. Ber.* **1971**, *104*, 1987–2001. (d) Effenberger, F.; Prossel, G.; Fischer, P. Kinetik und Mechanismus der Cycloaddition von *p*-Toluolsulfonylisocyanat an Enoläther; Kinetik der Epimerisierung und Umlagerung der gebildeten 4-Alkoxy-1-tosyl-3-alkyl-azetidinone-(2). *Chem. Ber.* **1971**, *104*, 2002–2012.

(25) (a) Gololobov, Y. G.; Linchenko, O. A.; Golding, I. R.; Galkina, M. A.; Krasnova, I. Y.; Garbuzova, I. A.; Petrovskii, P. V. Reactions of isocyanates with compounds containing active methylene groups in the presence of triethylamine. *Russ. Chem. Bull.* **2005**, *54*, 2398–2405. (b) Elvidge, J. A.; Judson, P. N.; Percival, A.; Shah, R. Preparation of Some Highly Polarised Ethenes by the Addition of Amines to Suitable Carbonitriles. *J. Chem. Soc., Perkin Trans. 1* **1983**, 1741–1744. (c) Mao, Y.; Lin, N.; Tian, W.; Han, X.; Han, X.; Huang, Z.; An, J. Design, Synthesis, and Biological Evaluation of New Diaminoquinazolines as *β*-Catenin/Tcf4 Pathway Inhibitors. *J. Med. Chem.* **2012**, *55*, 1346–1359. (d) Mekheimer, R. A.; Elgemeie, G. H.; Kappe, T. Synthesis of some novel azido- and tetrazoloquinoline-3-carbonitriles and their conversion into 2,4-diaminoquinoline-3-carbonitriles. *J. Chem. Res.* **2005**, 82–85. (e) Gololobov, Y. G.; Galkina, M. A.; Dovgan, O. V.; Guseva, T. I.; Kuzmintseva, I. Y.; Senchenya, N. G.; Petrovskii, P. V. Electrophilic 1,3-C→N^- and -N→ C^- migrations in saturated systems. *Russ. Chem. Bull.* **1999**, *48*, 1622–1627. (f) Capuano, L.; Zander, R. Basenkatalysierte Reaktionen aktiver Methylenverbindungen mit Isocyanaten, 2. Synthese von 2,4-Dioxo-3-azetidincarbonitrilen und 5-Cyanbarbitursäuren. *Chem. Ber.* **1973**, *106*, 3670–3676. (g) Linchenko, O. A.; Krasnova, I. Y.; Petrovskii, P. V.; Garbuzova, I. A.; Khrustalev, V. N.; Gololobov, Y. G. Novel reactions of arylmalonate carbanions. The reaction with phenyl isocyanate resulting in carbamates by 1,3-C→N migration of the ethoxycarbonyl group. *Russ. Chem. Bull.* **2007**, *56*, 1671–1674.

(26) (a) Ghattas, A.-B. A. G.; Jørgensen, K. A.; Lawesson, S.-O.; et al. Enamine Chemistry. XXVII. Reduction of Enaminones, Enaminothiones and Thioamides by $LiAlH_4$ and $NaBH_4$. *Acta Chem. Scand.* **1982**, *36b*, 505–511. (b) Berchtold, G. The Reaction of Enamines of Cyclic Ketones with Isocyanates. *J. Org. Chem.* **1961**, *26*, 3043–3044. (c) Ried, W.; Käppeler, W. Umsetzung von Cycloalken-aminen mit Phenyl-isocyanat bzw. Phenyl-senföl. *Liebigs Ann. Chem.* **1964**, *673*, 132–136. (d) Ferri, R. A.; Pitacco, G.; Valentin, E. Nucleophilic Behaviour of 1-Substituted Morpholino Ethenes. *Tetrahedron* **1978**, *34*, 2537–2543.

(27) (a) Nemoto, K.; Tanaka, S.; Konno, M.; Onozawa, S.; Chiba, M.; Tanaka, Y.; Sasaki, Y.; Okubo, R.; Hattori, T. Me_2AlCl-mediated carboxylation, ethoxycarbonylation, and carbamoylation of indoles. *Tetrahedron* **2016**, *72*, 734–745. (b) Hoberg, H.; Nohlen, M. Neuartige Ni^0-katalysierte Herstellung von 3-Cyclopentencarbonsäureaniliden aus Cyclopentenen und Phenylisocyanat. *J. Organomet. Chem.* **1990**, *382*, C6–C10.

(28) (a) Bokri, K.; Efrit, M. L.; Akacha, A. B. An Efficient Two-step Synthesis of Novel Substituted Pyrazolo[1,5,a]-[1,3,5]-Triazines and Pyrazolo[1,5-a]-[1,3,5] Triaziones. *Heterocycl. Lett.* **2015**, *5*, 679–685. (b) Shin, D.-W.; ChoiLee, I.-Y.; Lim, H.-J. Regioselective Synthesis of 3-Amino-4-arylisoxazol-5(4*H*)-ones. *Bull. Korean Chem. Soc.* **2010**, *31*, 3071–3072. (c) Khalafy, J.; Dilmaghani, K. A.; Soltani, L.; Poursattar-Marjani, A. The Synthesis of New 5-Aminoisoxazoles by Reaction of Thiocarbamoyl-cyanoacetates with Hydroxylamine. *Chem. Heterocycl. Compd.* **2008**, *44*, 729–734. (d) Metwally, M. A.; Abdel-Latif, E.; Amer, F. A. Synthesis and Reactions of Some Thiocarbamoyl Derivatives. *Sulfur Lett.* **2003**, *26*, 119–126. (e) Basheer, A.; Rappoport, Z. Thioenols and thioamides substituted by two *β*-EWGs. Comparison with analogous amides and enols. *J. Phys. Org. Chem.* **2008**, *21*, 483–491. (f) Fadda, A. A.; Latif, E. A.; EI-Mekawy, R. E. Synthesis of Some New Arylazothiophene and Arylazopyrazole Derivatives as Antitumor Agents. *Pharmacol. Pharm.* **2012**, *3*, 148–157. (g) Fadda, A. A.; Abdel-Latif, E.; El-Mekawy, R. E. Synthesis and molluscicidal activity of some new thiophene, thiadiazole and pyrazole derivatives. *Eur. J. Med. Chem.* **2009**, *44*, 1250–1256. (h) Barnikow, G.; Saeling, G. Reaktionen phosphono-substituierter CH-acider Thiocarbon-säureamide. *J. Prakt. Chem.* **1974**, *316*, 534–544.

(29) Schaumann, E.; Bäuch, H. G.; Sieveking, S.; Adiwidjaja, G. Cycloaddukte und Umlagerungsprodukte aus der Umsetzung von Isothiocyanaten mit Keten-acetalen. *Chem. Ber.* **1982**, *115*, 3340–3352.

(30) Kumar, K.; Konar, D.; Goyal, S.; Gangar, M.; Chouhan, M.; Rawal, R. K.; Nair, V. A. $AlCl_3$/Cyclohexane Mediated Electrophilic Activation of Isothiocyanates: An Efficient Synthesis of Thioamides. *ChemistrySelect* **2016**, *1*, 3228–3231.

(31) (a) Traube, W.; Eyme, A. Ueber Additionsreactionen der Carbodiimide. *Ber. Dtsch. Chem. Ges.* **1899**, *32*, 3176–3178. (b) Gompper, R.; Kunz, R. Tautomeriefähige Ketenaminale. Synthese von Chinolinen und 1.8-Naphthyridinen. *Chem. Ber.* **1965**, *98*, 1391–1398. (c) Resch, S.; Schneider, A.; Beichler, R.; Spera, M. B. M.; Fanous, J.; Schollmeyer, D.; Waldvogel, S. R. Naphthyridine derivatives as a model system for potential lithium-sulfur energy-storage applications. *Eur. J. Org. Chem.* **2015**, 933–937. (d) Kantlehner, W. Alk-1-ene-1,1-diamines. In *Science of Synthesis*, Vol. *24*; Meijere, A., Schaumann, E., Eds.; Thieme: Stuttgart, Germany, 2006; Chapter 24.2.17.1, pp 571–705. (e) Aggarwal, V.; Richardson, J. Sulfur ylides. In *Science of Synthesis*; Padwa, A., Bellus, D., Eds.; Thieme: Stuttgart, Germany, 2004; Vol. *27*, pp 21–104.

(32) Stephen, A. Über die Reaktion von C,H-aciden Verbindungen mit Carbodiimiden. *Monatsh. Chem.* **1966**, *97*, 695–702.

(33) Coady, D. J.; Norris, B. C.; Lynch, V. M.; Bielawski, C. W. Ionic Dithioester-Based RAFT Agents Derived from N-Heterocyclic Carbenes. *Macromolecules* **2008**, *41*, 3775–3778.

(34) (a) Kakehi, A.; Suga, H.; Okumura, Y.; Itoh, K.; Kobayashi, K.; Aikawa, Y.; Misawa, K. A New Approach to 1-Acyl-3-(substituted methylthio)thieno[3′,4′:4,5]imidazo[1,5-a]-pyridine Derivatives. *Chem. Pharm. Bull.* **2010**, *58*, 1502–1510. (b) Kakehi, A.; Suga, H.; Okumura, Y.; Nishi, T. One-pot Synthesis of 4-Substituted 5-Acylthieno[3,2-d]-Thiazole Derivatives. *Heterocycles* **2010**, *81*, 175–184. (c) Cuadro, A. M.; Alvarez-Builla, J.; Vaquero, J. J. Preparation of New Benzimidazole Derivatives from *N*-[(Methylthio)-thiocarbonylmethyl] Azinium Salts. *Heterocycles* **1989**, *29*, 57–65.

(35) Schaumann, E.; Grabley, F. F. Umsetzung von Phosphonat-Carbanionen mit Kohlenstoffdisulfid. *Liebigs Ann. Chem.* **1979**, 1715–1733.

(36) Gompper, R.; Wetzel, B.; Elser, W. 1.4-Dipole aus Enaminen und Schwefelkohlenstoff. *Tetrahedron Lett.* **1968**, *9*, 5519–5522.

(37) (a) Van Ausdall, B. R.; Glass, J. L.; Wiggins, K. M.; Aarif, A. M.; Louie, J. A Systematic Investigation of Factors Influencing the Decarboxylation of Imidazolium Carboxylates. *J. Org. Chem.* **2009**, *74*, 7935–7942. (b) Reitz, A. K.; Sun, Q.; Wilhelm, R.; Kuckling, D. The Use of Stable Carbene-CO_2 Adducts for the Polymerization of

Trimethylene Carbonate. *J. Polym. Sci., Part A: Polym. Chem.* **2017**, *55*, 820−829.

(38) Nemoto, K.; Onozawa, S.; Egusa, N.; Morohashi, N.; Hattori, T. Carboxylation of indoles and pyrroles with CO_2 in the presence of dialkylaluminium halides. *Tetrahedron Lett.* **2009**, *50*, 4512−4514.

(39) (a) Maloschik, E.; Mörtl, M.; Szekacs, A. Novel derivatisation technique for the determination of chlorophenoxy acid type herbicides by gas chromatography-mass spectrometry. *Anal. Bioanal. Chem.* **2010**, *397*, 537−548. (b) Schroth, W.; Andersch, J. Dimethylammonium-dimethylcarbamat(Dimcarb) − ein vorteilhaftes Reagens für die Willgerodt-Kindler-Reaktion. *Synthesis* **1989**, 202−204. (c) Xiong, W.; Yan, D.; Qi, C.; Jiang, H. Palladium-Catalyzed Four-Component Cascade Reaction for the Synthesis of Highly Functionalized Acyclic *O,O*-Acetals. *Org. Lett.* **2018**, *20*, 672−675. (d) Zhao, T.; Zhai, G.; Liang, J.; Li, P.; Hu, X.; Wu, Y. Catalyst-free *N*-formylation of amines using BH_3NH_3 and CO_2 under mild conditions. *Chem. Commun.* **2017**, *53*, 8046−8049. (e) Ghodsinia, S. S. E.; Akhlaghinia, B. A high-yielding, expeditious, and multicomponent synthesis of urea and carbamate derivatives by using triphenylphosphine/trichloroisocyanuric acid system. *Phosphorus, Sulfur Silicon Relat. Elem.* **2016**, *191*, 104−110. (f) Wright, H. B.; Moore, M. B. Reactions of Aralkyl Amines with Carbon Dioxide. *J. Am. Chem. Soc.* **1948**, *70*, 3865−3866.

(40) (a) Jangra, H.; Chen, Q.; Fuks, E.; Zenz, I.; Mayer, P.; Ofial, A. R.; Zipse, H.; Mayr, H. Nucleophilicity and Electrophilicity Parameters for Predicting Absolute Rate Constants of Highly Asynchronous 1,3-Dipolar Cycloadditions of Aryldiazomethanes. *J. Am. Chem. Soc.* **2018**, *140*, 16758−16772. (b) Zhang, J.; Chen, Q.; Mayer, R. J.; Yang, J.-D.; Ofial, A. R.; Cheng, J.-P.; Mayr, H. Predicting Absolute Rate Constants for Huisgen Reactions of Unsaturated Iminium Ions with Diazoalkanes. *Angew. Chem. Int. Ed.* **2020**, DOI: 10.1002/anie.202003029.

https://dx.doi.org/10.1021/jacs.0c01960
J. Am. Chem. Soc. XXXX, XXX, XXX−XXX